

Brian Genduso
 Structural Option
 Faculty Consultant – Dr. Linda Hanagan
 University of Cincinnati Athletic Center
 Cincinnati, Ohio



Courtesy of Bernard Tschumi Architects

Lateral System Analysis and Confirmation Design November 14, 2003

Executive Summary

The University of Cincinnati Athletic Center will be an 8-story, multi-use facility located in the heart of the university's athletic complex. The gravity framing system consists of typical steel composite wide flange beams with composite metal decking supporting one-way slab diaphragms. The lateral system is an unusual combination of a triangulated perimeter frame system called a diagrid, braced frames, "V" columns, foundation shear walls, anchor rods, and floor diaphragms.

Gravity and lateral loads were calculated using the Ohio Basic Building Code and ASCE Standard 7-98. Typical dead load is approximately 2500 kips per floor, live loads are usually 50 ksf. It was determined that West wind controls the lateral loading case for most but not all members.

Lateral load distribution through the building starts with the diagrid, which acts as a structural mesh, transferring forces in several directions. The rigid above-grade diaphragms help the diagrid carry shear down to the ground level, where it is picked up by the large V columns and braced frames. These two elements then transfer forces into the below-grade slabs and into the foundation shear wall and anchor rods, which safely spread the load into the surrounding soil.

A lateral analysis was performed with two separate computer programs. ETABS was used to find node displacement, V column support reactions, and member forces. STAAD was used to find braced frame stiffnesses. Results from both were combined through several spreadsheets and manual calculations to obtain stiffness element rigidities. The results of each individual analysis type are:

Analysis Type	Conclusion
Diagrid Story Drift	OK – High rigidity of the diagrid and its diaphragms. $\Delta_{actual} \approx \frac{1}{4} \Delta_{allowable}$
Ground Floor Story Drift	OK – Braced frames provide most resistance. $\Delta_{actual} \approx \frac{1}{2} \Delta_{allowable}$
Torsion	OK – Elliptical shape of building is well-suited to torsional effects.
Total Building Drift	OK – Even with torsion considered $\Delta_{actual} \approx \frac{1}{3} \Delta_{allowable}$
Overtopping	OK – Low building height and wide diagrid frame base prevent instability
Braced Frame Check	OK – Actual member size is slightly larger than calculated member sizes
Diagrid Member Check	OK – Max utilization factor of the evaluated members = 0.861 < 1.0

Overall, the building performs well under lateral loading conditions.

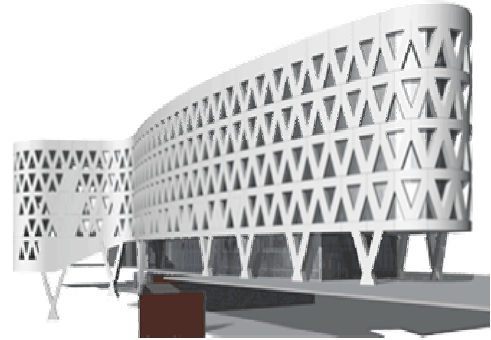
Index

Introduction	3
General Building Description	3
Gravity Framing System	3
Lateral System	4
Loads	5
Calculations	5
Wind	5
Seismic	6
Load Cases	6
Distribution	7
Above-grade	7
Below-grade	9
Lateral Analysis	10
Theory	10
Diagrid Story Drifts	12
Ground Floor Story Drift	14
ETABS Analysis	15
STAAD Analysis	20
Combined Results	21
Torsion	23
Total Building Drift	25
Overturning	25
Member Checks	26
Braced Frames	26
Diagrid Members	27
Conclusions	32
Appendices	
Appendix A – Gravity Load Calculations	
Appendix B – Wind and Seismic Load Calculations	
Appendix C – Node Numbering System	
Appendix D – ETABS Analysis Results	
Appendix E – STAAD Analysis Results	
Appendix F – Diagrid Member Checking Spreadsheets	

Introduction

General Building Description

The University of Cincinnati Athletic Center is an 8 story, 220,000 ft² multi-use facility to be located in the heart of UC's "Varsity Village" athletic complex. The building is designed to accommodate various sports-related activities all under one roof and to function as the social link and architectural centerpiece of a multi-stage athletic expansion plan. As such, it will be situated between two main sports facilities, the Nippert Football Stadium and the Shoemaker Center, with easy access to other sports fields and areas. The structure consists of 3 below-grade stories (levels 100-300) and 5 above-grade stories (levels 400-800), accommodating offices, public meeting areas, computer labs, locker rooms, treatment areas, and other related athletic spaces.



Gravity Framing System

The floor framing system consists of typical steel composite wide flange beams with composite metal decking supporting one-way slab diaphragms. Most connections are shear only, though some elements framing into full height columns near the atrium are designed with moment connections to support atrium walkways. The layout is irregular due to the highly curved shape of the building, however, the N-S direction spacing is typically 9' o.c. within 27' bays. A representative above-grade framing plan is show in Figure 1.

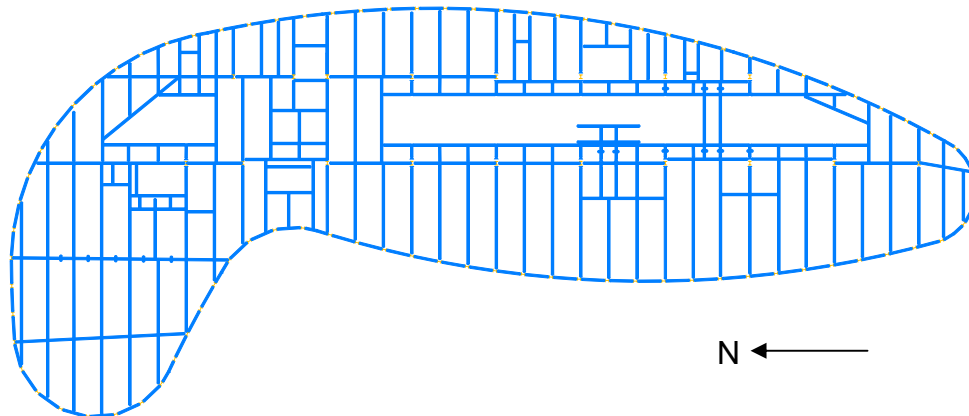


Figure 1: Main framing areas

Lateral System

Diagrid and Diaphragms

The above-grade enclosure of the UC Athletic Center is a triangulated, curved perimeter frame system called a diagrid. The diagrid acts as a rigid shell, and for structural purposes can be considered a very thin, deep beam. It is composed of wide flange rolled sections welded or bolted for full restraint. The steel will be covered with concrete or similar material to produce a monolithic appearance. Between the beams are triangular window glazings. A rendering of a typical diagrid connection is shown in Figure 2. The above-grade diaphragms are 6.5" reinforced concrete slabs on metal deck, supported by steel framing. There are numerous slab openings, including the main atrium and several elevator and stair shafts.

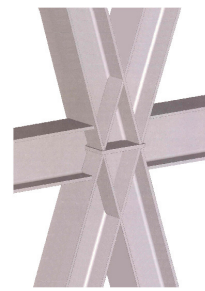


Figure 2

Braced Frames

There are four types of braced frames. Two of them, labeled BF2 and BF3, are light braced frames around the atrium staircase. They both span from Level 100 to Level 400 (ground floor) and provide lateral support for the staircase only. The other two, labeled BF1 and BF4, are heavy braced frames to resist lateral movement for the entire building. Two BF1s brace against E-W deflection around an elevator shaft in the northern half of the building, while the lone BF4 braces against E-W deflection in the southern half. Frame elevations are shown below in Figure 3.

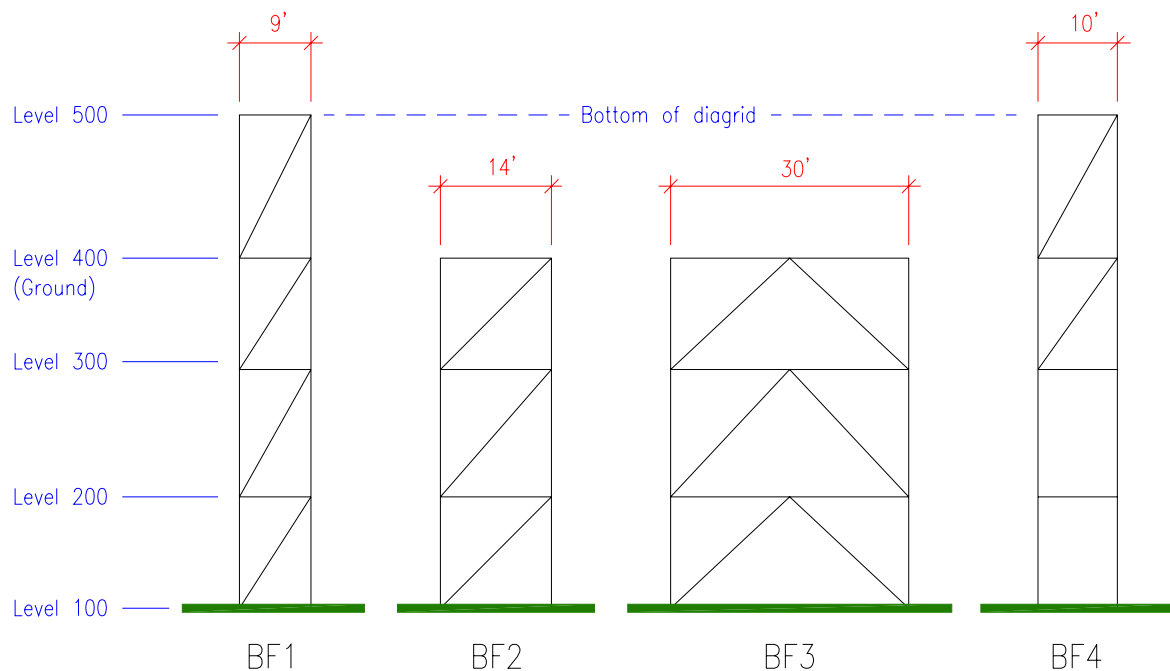


Figure 3: Braced Frame Elevations

Columns

There are two kinds of columns found in the UC Athletic Center. Within the perimeter of the building are two rows of full height vertical columns, supporting the floor and partition gravity loads of the interior bays. Between Levels 300 and 500 are large “V” columns which are rigidly connected to both the diagrid and the substructure. Though their primary function is to carry gravity load from the diagrid, they also play a significant role in the transfer of lateral forces from the bottom of the diagrid to ground level. They are made of either heavy wide flange rolled shapes or built-up boxes, and sit on single below-grade columns. A rendering of a V column is shown in Figure 4.

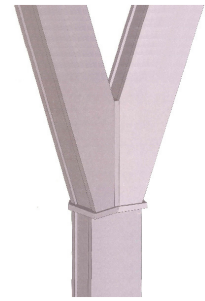


Figure 4

Foundation Shear Walls and Diaphragms

The foundation utilizes a combination of spread footings and drilled piers, set into sound gray shale. Reinforced concrete shear walls below grade serve as the retaining walls as well and are typically 1’6” thick. They are rectangular in plan and therefore do not carry the loading from the curved above-grade floors. They do, however, work with the below-grade diaphragms to resist shear forces. There are 16 threadbar anchor rods embedded in the foundation walls to resist shear. As in the upper floors, the foundation diaphragms are 6.5” reinforced concrete slabs on metal deck.

Loads

Calculations

Building loads were obtained using ASCE 7-98 Standard, which is referenced in the 1998 Ohio Basic Building Code. The loading can be split into two main categories, gravity loads and lateral loads. This report focuses on the lateral loading of the building due to wind and seismic forces, however gravity load calculations and summaries as found in Technical Report #1 are included in Appendix A.1 for reference.

Wind Loads

Wind loads are based on a 90mph basic wind speed, exposure B, and an importance factor of 1.15. Though the shape of the building is unusual, it is assumed that the building can be modeled as a simple rectangular box, 5 stories high. The high roof is not taken into consideration for purposes of simplicity. Calculations are found in Appendix B.1. Wind pressures gradients are evaluated in both the N-S and E-W directions, as found in Appendix B.2. The summation of story shear is evaluated in Appendix B.3. They are summarized in graphical format in Figures 5 and 6 below, with total base shear equal to 122.5 kips N-S, 408.3 kips E-W.

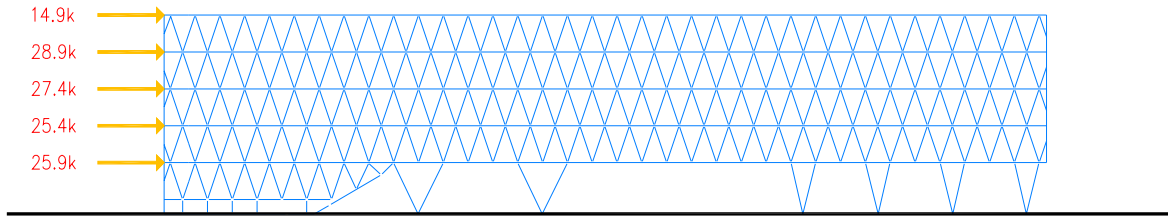


Figure 5: Wind shear in N-S direction

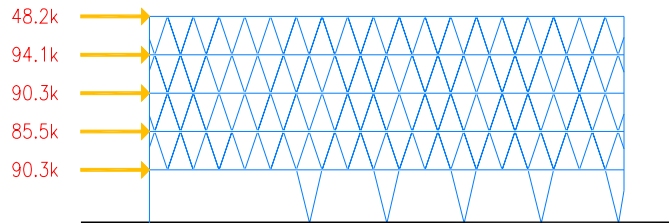


Figure 6: Wind shear in E-W direction

Seismic Loads

The governing code used in the structural design of the UCAC is the 2002 OBBC, which is adapted from the IBC 2000. IBC 2000 references ASCE 7, and therefore seismic analysis was performed using ASCE 7-98 for consistency with the wind analysis. The design is based on Seismic Use Group II, Site Class B, and an importance factor of 1.25. Using these provisions, the building fell under Seismic Design Category A, and therefore the story shear could be calculated as $F_x=0.01 \cdot g$. Calculations to determine the SDC are found in Appendix B.4. Seismic story shear is the same in both directions, summarized in Figure 7 below. The total base shear equal to 392 kips.

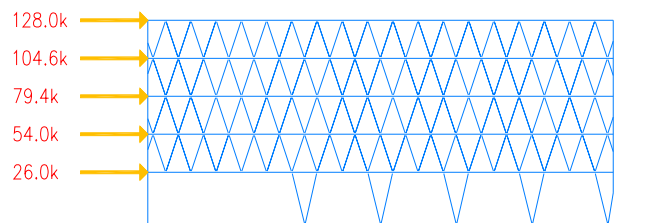


Figure 7: Seismic shear in both directions

Load Cases

The wind and seismic base shear calculated in the previous section are very similar for the E-W direction, while seismic appears to control in the N-S direction. However, the two load types behave quite differently on the diagrid itself. In the case of wind, story by story distribution of the forces is fairly even. In the seismic case, the highest forces occur at the top of the structure and decrease towards the ground floor (Level 400). This implies that wind will be the controlling load case for lower story members, while seismic is likely to control for upper story members.

For purposes of keeping the amount of computer modeling and calculations to a minimum only one load case will be evaluated. It is assumed that a thorough study of one particular loading situation will be sufficient to understand the concepts behind the lateral design, and that additional loading situations would simply reinforce those concepts. With that in mind, the West wind situation was chosen as the overall controlling load case. This case provides the highest base shear, which will be critical in evaluating Level 400 story drift and the braced frames. It also allows an opportunity to look at unbalanced loading and torsion issues.

For the West wind load situation, there are four applicable cases from the Basic Load Combinations found in section 2.3 of ASCE 7-98. They will be used to check member sizes in subsequent sections. They are:

Case 1: $1.4D$

Case 2: $1.2D + 1.6L + 0.5S$

Case 3: $1.2D + 0.5L + 1.6S$

Case 4: $1.2D + 1.6W + 0.5L + 0.5S$

Where D = Dead Load, L = Live Load, S = Snow Load, W = Wind Load

Distribution

Above-grade

The distribution of lateral loads through the structure is looked at in the E-W direction since it is the critical case.

First, the diagrid is loaded by wind or seismic forces. The shear created by the load is transferred from a higher story to lower story through the diagonal members. When these forces reach the floor level below, horizontal beams help pick up part of the load along with diagonal members in the story below (Figure 8). This redundant geometry can be considered a continuous structural mesh around the entire perimeter. It might be easier to visualize the diagrid as a trampoline. When force is applied to a trampoline the load is carried by the mesh in all directions. Of course, the diagrid is much more rigid than a trampoline, but the analogy still holds true!

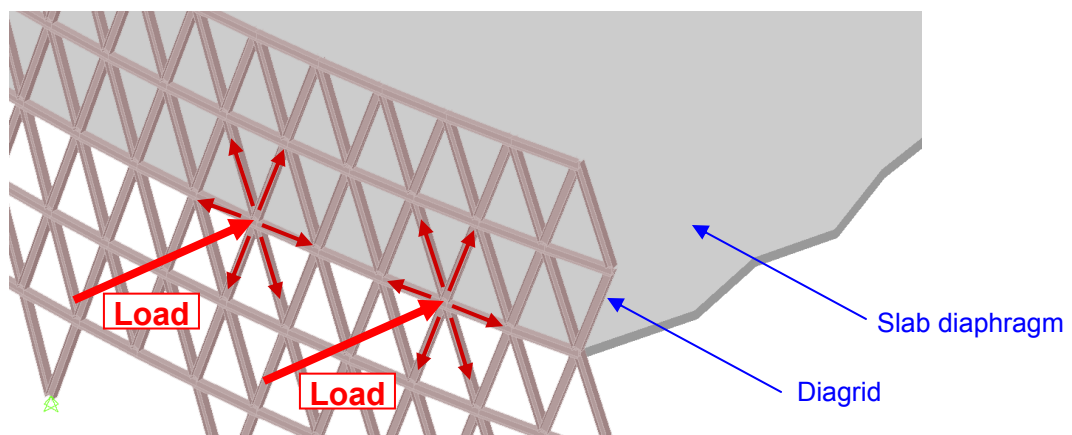


Figure 8: Load path into diagrid

The high rigidity of the diagrid acts with the help of the floor diaphragm as well. Shear forces are transferred through the floor slab. Even with the large atrium running N-S through the middle of the building, there is enough slab around the perimeter and through the middle of the diaphragm to transfer the shear. This is reinforced with additional rebar that is added to the slab in critical shear sections. A diagram of the shear transfer through the diaphragm is shown in Figure 9.

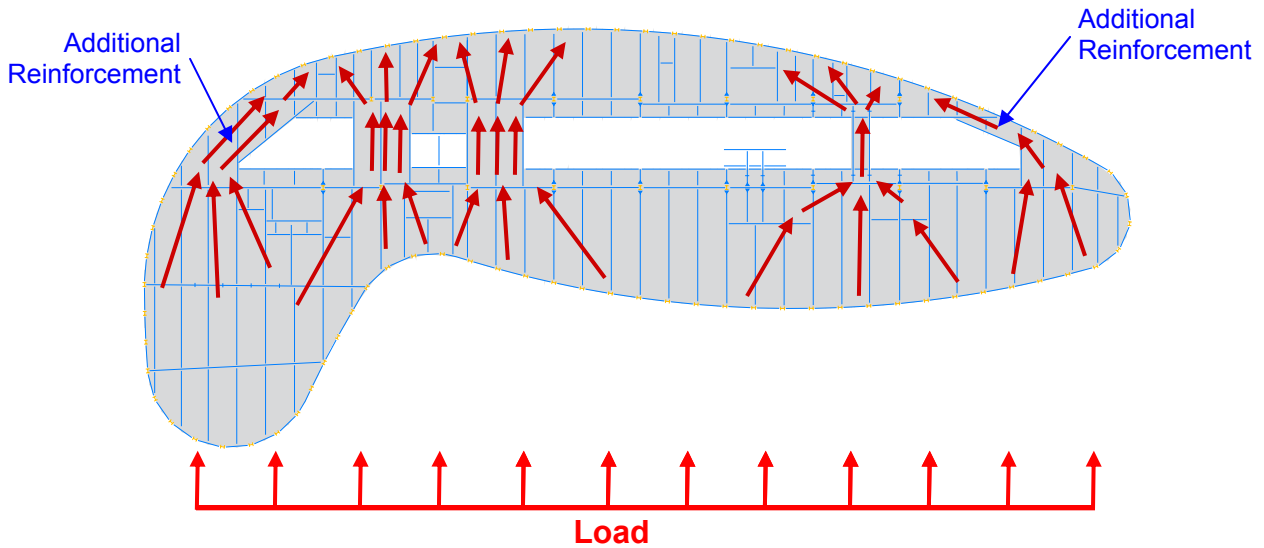


Figure 9: Shear transfer through the diaphragm

When lateral load reaches Level 500, the bottom of the diagrid, it is picked up by the braced frames and the V columns. The braced frames carry most of the lateral load due to their higher stiffness and orientation parallel to the load. They also help resist torsion, because they are located on opposite sides of the building. The V columns also play a large role in resisting torsion. Because of the building's semi-elliptical shape, the V columns are arranged around the perimeter in such a way that their strong axis is nearly perpendicular to the center of rigidity, which will provide the maximum resistance to torsion forces. Three of the larger V columns under auditorium at the north end of the building sit on pilasters and are considered roller supported. Therefore, no lateral loads are transferred at the northern end of the building. The forces resisted by each frame and column can be evaluated by the stiffness method. Figure 10 shows the shear transfer elements at ground level.

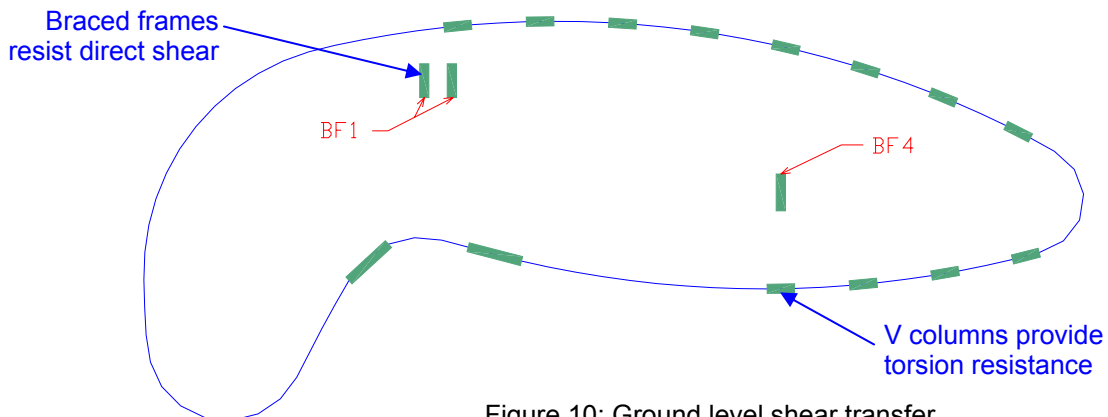


Figure 10: Ground level shear transfer

Below-grade

At Level 300 the lateral load begins to be picked up by the ground floor shear walls and diaphragm. At each subsequent level more and more of the lateral load is taken out of the braced frames and perimeter columns and transferred into the below-grade shear walls and diaphragms. This theory is validated by observing that the lower braced frame diagonals in BF1 are actually smaller member sections than the upper braced frame diagonals. In fact, BF4 does not even need diagonal members below Level 300. If lateral load is not being taken out at each level the lower diagonal members would need to be greater than the upper members.

The load transferred out of the braced frames and columns then flows into the foundation retaining walls. These shear walls transfer some of the shear forces safely into the surrounding soil. The rest of the forces are taken down into the footings. Because the UC Athletic Center will connect to an existing structure below grade at its southern end, anchor rods embedded into sound gray shale at that end reinforce the shear walls and mitigate forces from reaching the existing structure. The rods also tie down the building in case of wind uplift on the foundation wall.

Finally, the column footings and piers transfer the remaining lateral loads into the soil below the structure. By this point much of the load has been resisted by the shear walls and anchor rods. The only lateral-induced loads left are the uplifts on the columns of BF1 and BF4. These forces are resisted by the concrete piers which are set into sound rock below. The below-grade distribution of forces is shown in Figure 11 with a section view of the building. The section cuts through BF4.

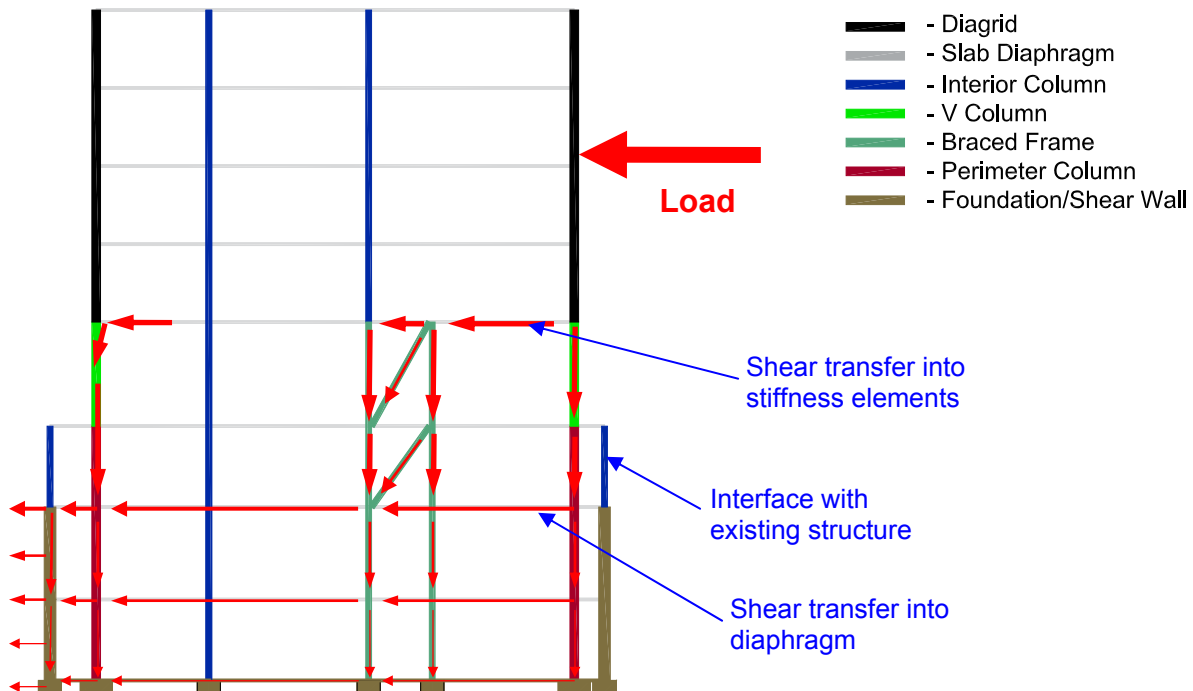


Figure 11: Below-grade lateral force distribution

Lateral Analysis

Theory

Much time was spent assessing the lateral behavior of the UC Athletic Center and how it should be modeled for a lateral analysis. In the end, though the building could have been simplified enough to perform hand calculations, it was determined that a more accurate 3-dimensional computer model is the best method of analysis. The flow of forces through the unique lateral system of the diagrid is difficult to visualize compared to a traditional box-shaped building. As you will see by the graphic-intensive nature of this report, a 3D model presents a clearer picture of the structure's response to load, yet also provides an opportunity to check the results of the output using manual methods. Learning a new structural analysis software program is an additional benefit.

ETABS was chosen to perform the analysis. ETABS is a non-linear, finite element pre and post-processing software package enhanced for the structural analysis of buildings. The benefits of ETABS include dxf file import, unlimited node and member input, graphical and tabular output options including forces and displacements, and pre-loaded steel member section properties.

Even with these computational capabilities, the procedure for modeling the structure in ETABS was simplified. Only the above-grade diagrid structure was included. Foundation shear walls and braces would have to be a separate analysis. The procedure was done so that all of the separate required analyses (i.e. story drift, total drift, torsion, overturning) could be modeled individually. For instance, the diagrid drifts were treated separately from Level 400 drifts because of potential for torsion effects and disproportionately high Level 400 drifts. Also, because it was not determined how to accurately model braced frames and V columns at the same time, the stiffnesses of the V columns were assessed first, the braced frames second. The two were then put together to obtain total stiffness at the ground level.

The model was constructed in the following fashion:

It was first drawn in 3D AutoCAD using the column positions, floor heights, and member lengths found on the drawings. Figure 12 shows the model skeleton.

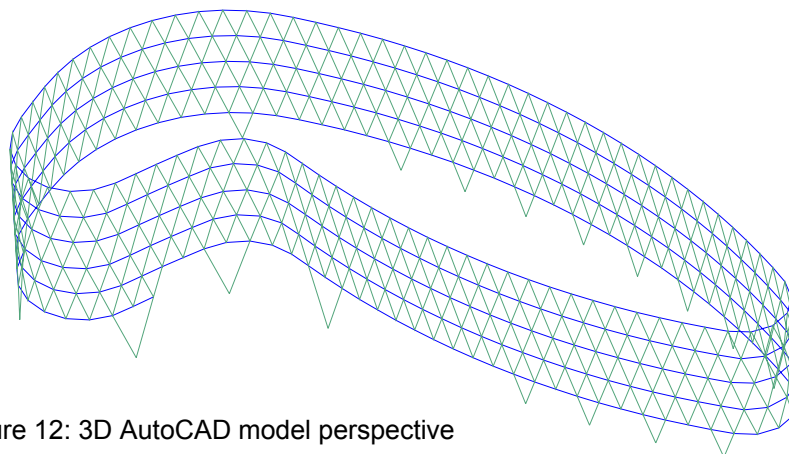


Figure 12: 3D AutoCAD model perspective

It was then imported into ETABS using an AutoCAD dxf file. Rigid diaphragms were added to model the floor framing and slab system and to stabilize the structure against unnecessary P-delta effects. All elements were modeled with their true member sections as called out on the drawings. A rendered ETABS image of the diagrid and diaphragms is shown in Figure 13.

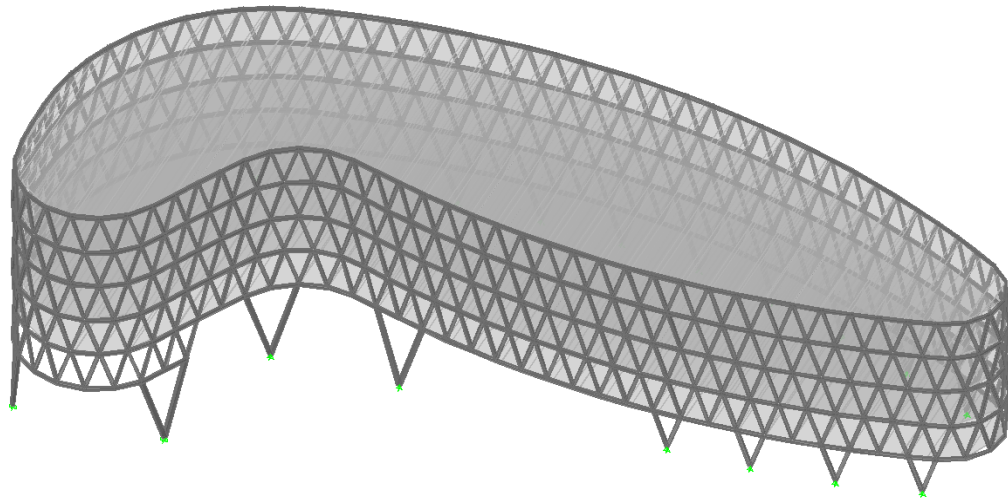


Figure 13: ETABS model perspective

The bottom points of the V columns were given support conditions as necessary. Most of the nodes are pinned to represent a V column connected to a single column at ground level. The three previously mentioned V columns under the auditorium are given roller supports. All supports are numbered for easy reference in the future (Figure 14). The structure is now completely modeled.

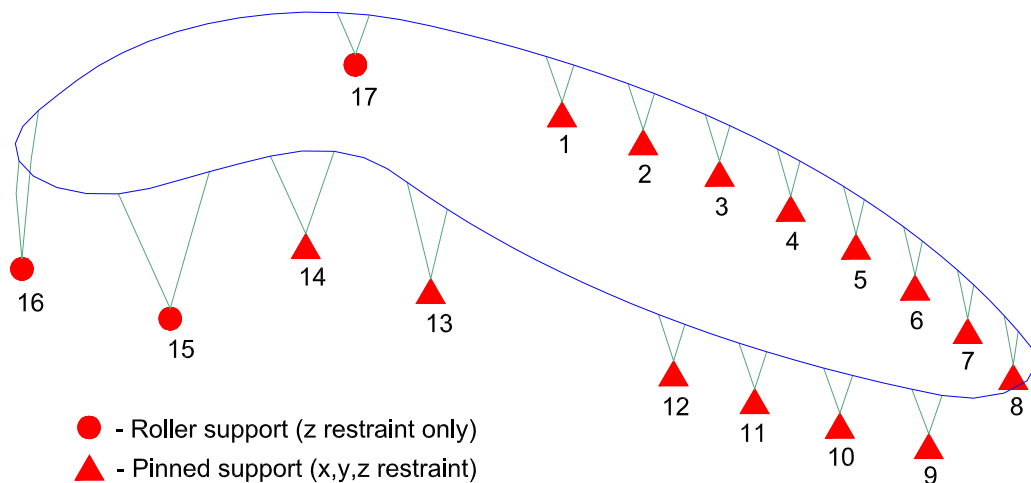


Figure 14: Support conditions

Diagrid Story Drifts

To estimate diagrid story drifts, unfactored wind load was added to the structural model as a uniform line load at each floor diaphragm in the west direction. The values of these loads were obtained from the wind load calculations in a previous section. Windward and leeward loads were separated and applied on their respective sides. Tabular and visual summaries of distributed loads are included below (Table 1 and Figure 15). For full results see Appendix B.

E-W Direction Windward		E-W Direction Leeward	
Level	Story Dist. Load (plf)	Level	Story Dist. Load (plf)
Roof	99	Roof	61
800	191	800	123
700	178	700	123
600	162	600	123
500	158	500	143

Table 1: Wind load values

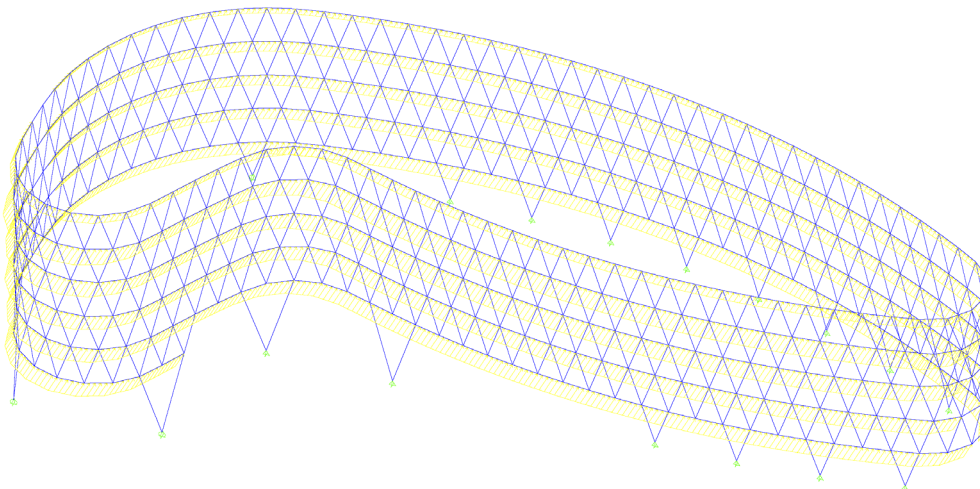


Figure 15: Applied wind loads

The model was analyzed and the west direction node displacement output was obtained from ETABS. Because of the complexity and size of the output tables, a method to visualize the displacement values was developed. All nodes were numbered along along Level 500 (bottom of diagrid, see Appendix C for numbering system). Every third node along the perimeter and the nodes directly above at Level 700 and Level 900 were evaluated for displacement. Displacements at Level 600 and Level 800 were interpolated. These displacements were referenced from Level 500 to determine net displacement. The results are tabulated in an Excel spreadsheet (Table 2) and each displacement is colorized by its magnitude. At the bottom of the table the maximum story drifts are calculated for each level. Furthermore, the colors from the spreadsheet are superimposed onto an AutoCAD frame of the diagrid, shown below in Figure 16.

Node	Total Displacement			Net Displacement			
	Level 500	Level 700	Level 900	Level 600	Level 700	Level 800	Level 900
1	1.425	1.527	1.586	0.051	0.102	0.132	0.161
4	1.357	1.464	1.524	0.054	0.107	0.137	0.167
7	1.274	1.388	1.450	0.057	0.114	0.145	0.176
10	1.191	1.311	1.374	0.060	0.120	0.152	0.183
13	1.107	1.233	1.298	0.063	0.126	0.159	0.191
16	1.021	1.154	1.221	0.067	0.133	0.167	0.200
19	0.936	1.075	1.144	0.070	0.139	0.174	0.208
22	0.851	0.997	1.068	0.073	0.146	0.182	0.217
25	0.767	0.919	0.992	0.076	0.152	0.189	0.225
28	0.687	0.845	0.919	0.079	0.158	0.195	0.232
31	0.676	0.835	0.909	0.080	0.159	0.196	0.233
34	0.746	0.900	0.973	0.077	0.154	0.191	0.227
37	0.824	0.972	1.043	0.074	0.148	0.184	0.219
40	0.905	1.046	1.116	0.071	0.141	0.176	0.211
43	0.99	1.123	1.191	0.068	0.135	0.169	0.203
46	1.072	1.200	1.267	0.064	0.128	0.162	0.195
49	1.156	1.279	1.343	0.062	0.123	0.155	0.187
52	1.242	1.358	1.420	0.058	0.116	0.147	0.178
55	1.327	1.436	1.497	0.055	0.109	0.140	0.170
58	1.411	1.514	1.573	0.052	0.103	0.133	0.162
61	1.493	1.590	1.647	0.049	0.097	0.126	0.154
64	1.570	1.659	1.713	0.045	0.089	0.116	0.143
67	1.613	1.701	1.756	0.044	0.088	0.116	0.143
70	1.635	1.722	1.776	0.044	0.087	0.114	0.141
73	1.634	1.721	1.775	0.044	0.087	0.114	0.141
76	1.599	1.690	1.744	0.046	0.091	0.118	0.145
79	1.519	1.614	1.670	0.048	0.095	0.123	0.151
82	1.466	1.565	1.623	0.050	0.099	0.128	0.157
Max				0.080	0.080	0.117	0.117

Color Key	
in.	
0 - 0.06	0.051
0.06 - 0.11	0.102
0.11 - 0.14	0.132
0.14 - 0.17	0.161
0.17 - 0.20	0.191
0.20 - 0.23	0.232
0.23 - 0.24	0.233

Table 2: Diagrid node displacement chart

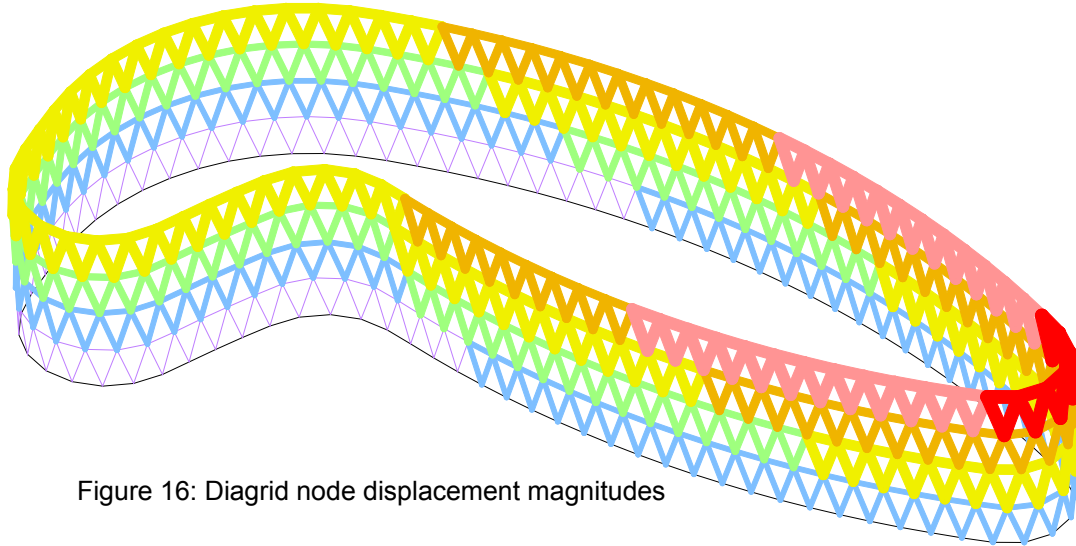


Figure 16: Diagrid node displacement magnitudes

As you can see from Figure 16, the diagrid net displacements are very consistent at the north end of the building. This is no doubt due to the projecting “hook” in the E-W direction, which provides stability against the west wind. At the south end of the building displacement increases substantially. The further away from the stable north end the member is, the more it is displaced. The southern top tip of the building moves 0.233 in., compared to 0.14 in. at the northern tip.

The allowable story drift must be calculated in order to compare it to the maximum story drifts at the bottom of Table 2. Each level in the diagrid is 13'-6" high. From the building specifications, allowable story wind drift is $L/350$. The calculated allowable drift is therefore $(13.5') \cdot (12 \text{ in./ft.}) / 350 = 0.463 \text{ in.}$

Wind Drifts	Level 600	Level 700	Level 800	Level 900
Allowable	0.463	0.463	0.463	0.463
Actual	0.080	0.080	0.117	0.117
Outcome	OK	OK	OK	OK

Table 3: Allowable story drift comparison

Therefore, all diagrid story drifts (Levels 500-800) are within the allowable drift.

Ground Floor Story Drift

To estimate ground floor (Level 400) story drifts in the west direction, a more complicated process was necessary. As explained in the Lateral System Theory section, an adequate way to connect the braced frames to the diagrid diaphragm in ETABS was not found, therefore only the V columns were modeled. Stiffnesses for the V columns in the x direction using ETABS were found first. An alternate method was then used to determine stiffnesses of the braced frames. Finally, results from the two analyses were combined to obtain an overall stiffness for Level 400, which was used to calculate story drift.

ETABS Analysis

The ETABS model was analyzed and Level 500 deflections were obtained. The results can be found in Appendix D.1, with support nodes highlighted in green, minimum displacements in yellow, and maximum displacements in red. As you can see from the node displacement results (column "UX"), nodal displacement varies from 0.667 to 1.637. Since the rigid diaphragm in the model keeps the nodes consistently spaced in the xy plane under loading, this means that the building is undergoing slight torsion. This is further reinforced at the bottom of Appendix D.1, where the diaphragm results show that level 500 (story 1) undergoes a -0.00026 rad rotation about the positive z axis (column "RZ"). This rotation is exaggerated below in Figure 17.

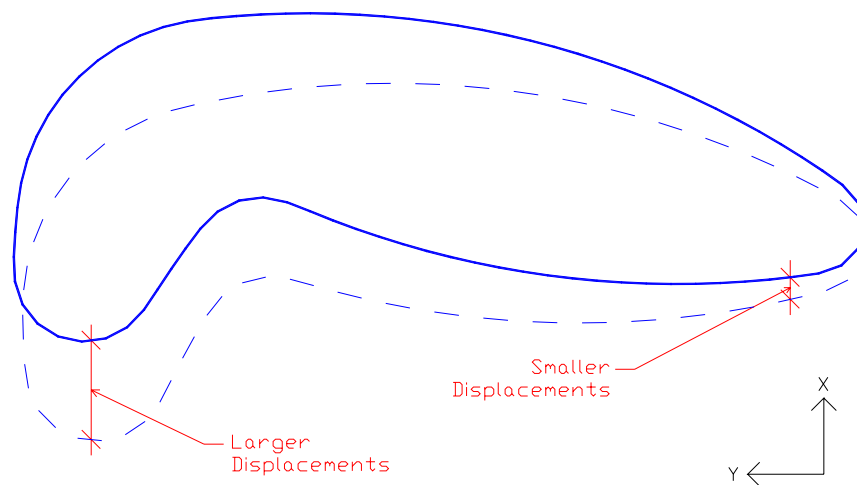


Figure 17: Building rotation

Since the building is undergoing torsion, the x direction stiffnesses that could be obtained from this model would be inaccurate. This is because torsion introduces additional forces in the V columns (stiffness elements) based on their distance from the structure's center of rigidity. The center of rigidity is where the resultant load must act to eliminate torsion. The loading condition will be remodeled in an iterative manner until torsion is substantially reduced.

To do this, first the support reactions in the x direction are obtained from ETABS (Appendix D.2). Then the distances of the V column supports from the northernmost tip of the building (d_{north}) are found from the drawings. Figure 18 highlights the stiffness elements in green and their (d_{north}) distances. These two values, along with the support node displacements from Appendix D.1, are used in an Excel spreadsheet to calculate Δ_{unit} , rigidity (k), and $k*d_{\text{north}}$ for all pinned columns. The three roller-supported columns do not carry any x direction force and are therefore neglected. The results are displayed in Table 4.

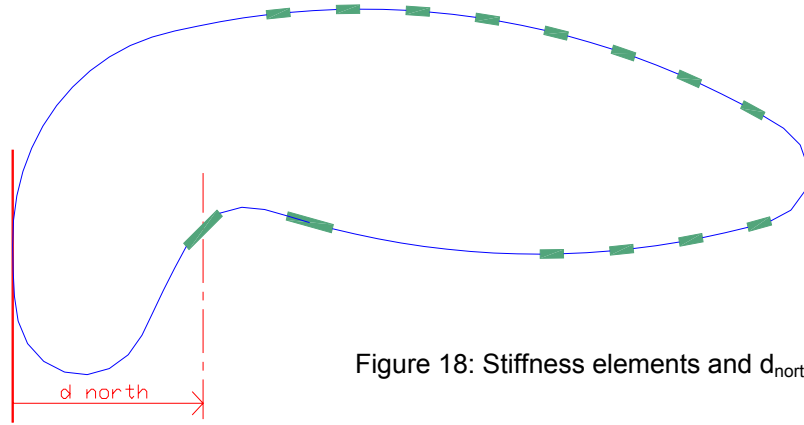


Figure 18: Stiffness elements and d_{north}

Support	Node	Reaction	Displacement	Δ_{unit}	Rigidity (k)	d_{north}	$k*d_{north}$
		kips	in.	in.	kips/in.	ft.	kips
1	54	25.36	1.299	0.0512	19.52	103	24130
2	51	3.65	1.214	0.3326	3.01	130	4690
3	48	-0.28	1.129	-4.0321	-0.25	157	-467
4	45	3.08	1.044	0.3390	2.95	183	6479
5	42	12.85	0.960	0.0747	13.39	210	33731
6	39	27.99	0.878	0.0314	31.88	236	90282
7	36	46.69	0.799	0.0171	58.44	261	183020
8	33	66.09	0.722	0.0109	91.54	286	314156
9	26	14.74	0.740	0.0502	19.92	288	68840
10	23	4.15	0.824	0.1986	5.04	262	15834
11	20	-0.05	0.908	-18.1600	-0.06	235	-155
12	17	4.53	0.994	0.2194	4.56	208	11375
13	7	45.04	1.275	0.0283	35.33	115	48749
14	2	265	1.408	0.0053	188.21	73	164872
Sums		518.84			473.46		965537

Table 4: Rigidity calculations

The negative stiffnesses are likely a result of building geometry, and should be resolved when the load is closer to the center of rigidity.

The new center of rigidity in the x direction is calculated by dividing the sum of $k*d_{north}$ values by the sum of k values, which is the total stiffness in the x direction.

$$\text{Center of Rigidity} = \frac{\sum(k*d)}{\sum k} = \frac{965537}{473.46} = 2039 \text{ in.} = 170 \text{ ft.}$$

The resultant load from the distributed wind loads acts along the geometric center of the building's N-S length, or $300'/2 = 150'$ from the northernmost tip. The actual center of rigidity for the stiffness elements is at 170', a distance of 20' from the resultant load. This accounts for the diaphragm rotation at level 500. Since rigidity is concentrated toward the southern end of the building, it is to be expected that the building's northern end is displaced more.

Now that a center of rigidity has been calculated, the next iteration is to modify the wind load to act along the center of rigidity. The distributed load used in the first iteration is resolved into a single point load, applied at Level 500. The magnitude of the point load is taken from the sum of the reactions found in Table 4. This is shown in Figure 19.

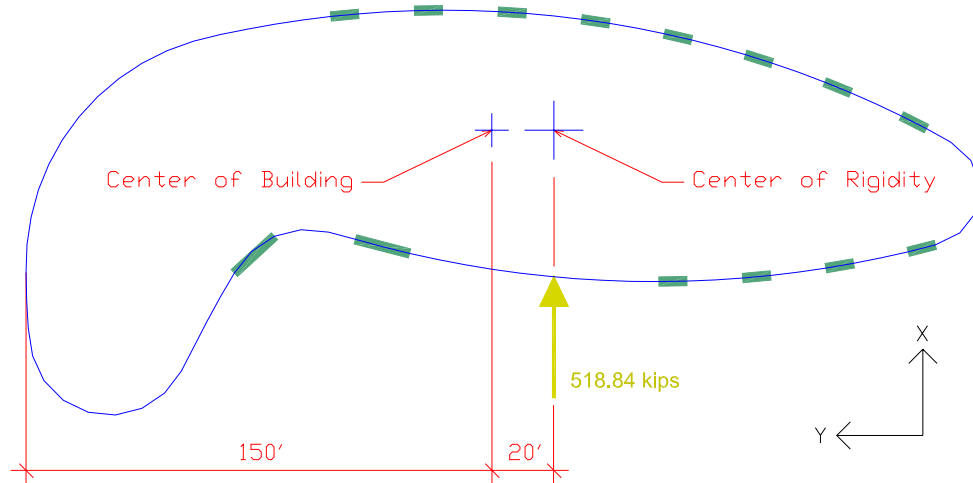


Figure 19: Load recentered at $d_{north} = 170'$

An ETABS analysis is run. See Appendix D.3 for reactions and Appendix D.4 for node displacements and rigid diaphragm rotation. The same process is used again to try and obtain an even more accurate estimation of the center of rigidity location. Results are obtained using the spreadsheet in Table 5.

Support	Node	Reaction	Displacement	Δ_{unit}	Rigidity (k)	d_{north}	$k \cdot d_{north}$
		kips	in.	in.	kips/in.	ft.	kips
1	54	20.76	1.141	0.0550	18.19	103	22488
2	51	3.10	1.090	0.3516	2.84	130	4437
3	48	0.85	1.038	1.2212	0.82	157	1543
4	45	5.32	0.987	0.1855	5.39	183	11837
5	42	15.93	0.937	0.0588	17.00	210	42843
6	39	31.96	0.887	0.0278	36.03	236	102041
7	36	51.83	0.839	0.0162	61.78	261	193482
8	33	72.10	0.793	0.0110	90.92	286	312039
9	26	21.78	0.804	0.0369	27.09	288	93621
10	23	9.68	0.854	0.0882	11.33	262	35637
11	20	3.02	0.906	0.3000	3.33	235	9400
12	17	5.45	0.957	0.1756	5.69	208	14214
13	7	36.90	1.127	0.0305	32.74	115	45184
14	2	240.17	1.207	0.0050	198.98	73	174307
Sums		518.85			512.15		1063074

Table 5: Rigidity calculations for $d_{north} = 170'$

As suspected, the rigidities are all positive now that the load has been moved. The new center of rigidity in the x direction is again calculated by dividing the sum of $k*d$ values by the sum of k values.

$$\text{Center of Rigidity} = \Sigma(k*d)/\Sigma k = 1063074/512.15 = 2076 \text{ in.} = 173 \text{ ft.}$$

This new center of rigidity is now only 3 feet away from the previous center of rigidity, yet the rotation of the rigid diaphragm as found in Appendix D.4 remains fairly high, -0.00016 rad as opposed to -0.00026 rad from the first load situation. It is obvious that the method developed above is not going to converge at the true center of rigidity. This might be due to the 2D nature of V column stiffness. In this method only stiffness in the x direction has been considered, when in fact a large portion of the structure's resistance is being resolved in the y direction. The above method, however, gives us a starting point to proceed further. By using a simple linear relationship, a new trial center of rigidity is obtained. The process is now based on the relative differences in diaphragm rotation. New trial locations are calculated, again iteratively, until a reasonable accuracy is found.

$$\frac{(-0.00026 - (-0.00016\text{rad}))}{-0.00026\text{rad}} = \frac{20'}{d_c}, \quad d_c = 52.0'$$

The term d_c is the distance from the center of the building geometry ($150'$ from the northernmost tip). Therefore, the load will need to be moved an additional $52'-20' = 32'$ south for the next trial.

Another ETABS analysis is performed with the load centered at $d_{\text{north}} = 150'+52' = 202'$, as shown in Figure 20. See Appendix D.5 for node displacements and rigid diaphragm rotation.

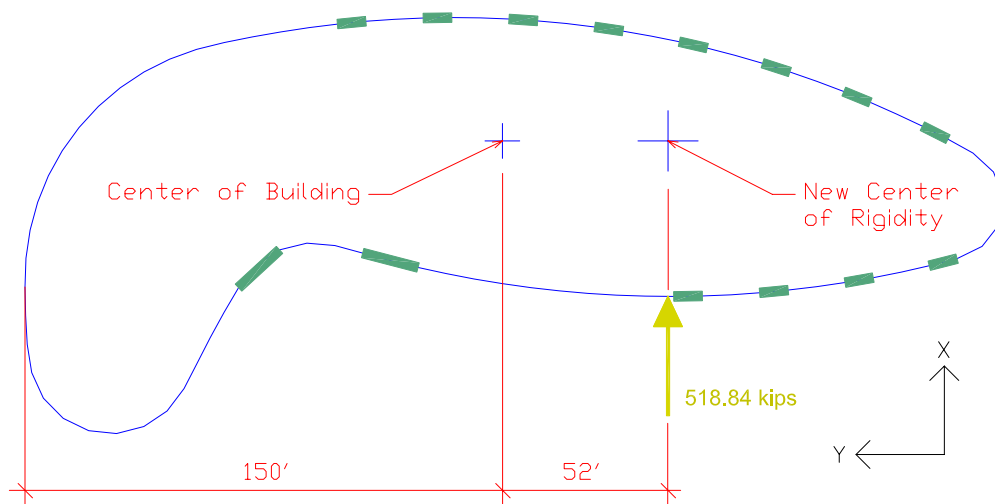


Figure 20: Load recentered at $d_{\text{north}} = 202'$

Torsion is now limited to -0.00007 rad as opposed to -0.00016 rad. One more iteration should be sufficient to obtain a direct load (i.e. no torsion) case. Again, a linear relationship is established.

$$\frac{(-0.00026 - (-0.00007\text{rad}))}{-0.00026\text{rad}} = \frac{52'}{d_c}, \quad d_c = 71.2'$$

Another ETABS analysis is performed with the load centered at $d_{\text{north}} = 150' + 71.2' = 221.2'$, as shown in Figure 21. See Appendix D.6 for node displacements and rigid diaphragm rotation.

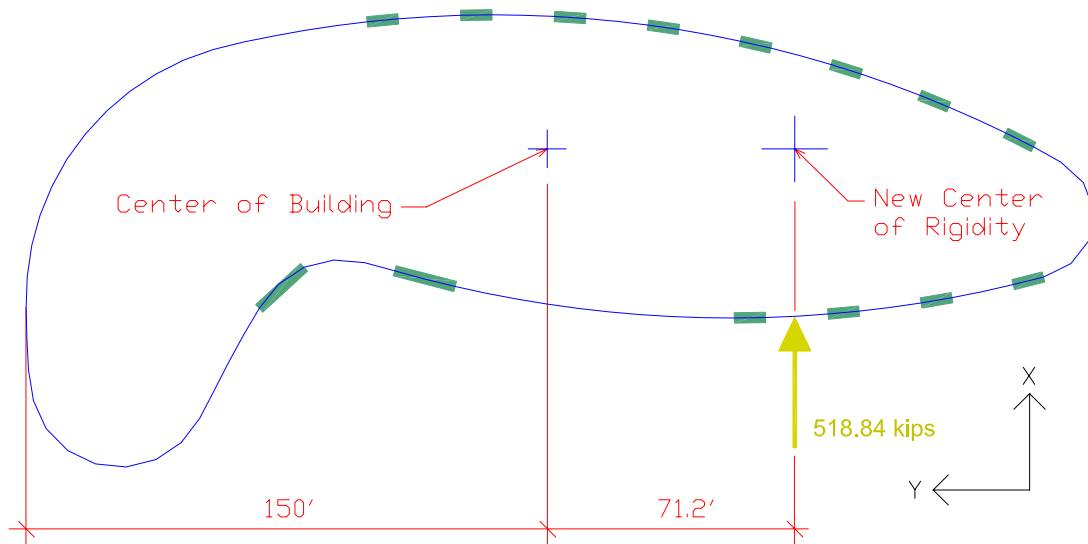


Figure 21: Load recentered at $d_{\text{north}} = 221.2'$

Torsion is now limited to -0.00001 rad, which is sufficiently small to consider the load as acting through the center of rigidity in the x direction. Now that the center of rigidity is found, the reactions in Appendix D.7 can be inputted along with the displacements into a table similar to those used above to obtain k for the V columns (Table 6). Since the load is considered to be acting through the center of rigidity, the x direction rigidity calculated in Table 6 for each V column is final.

Support	Node	Reaction	Displacement	Δ_{unit}	Rigidity (k)
		kips	in.	in.	kips/in.
1	54	14.18	0.930	0.0656	15.25
2	51	2.26	0.927	0.4102	2.44
3	48	2.40	0.925	0.3854	2.59
4	45	8.56	0.922	0.1077	9.28
5	42	20.58	0.919	0.0447	22.39
6	39	38.18	0.916	0.0240	41.68
7	36	60.11	0.914	0.0152	65.77
8	33	83.11	0.911	0.0110	91.23
9	26	34.19	0.912	0.0267	37.49
10	23	17.92	0.915	0.0511	19.58
11	20	7.40	0.917	0.1239	8.07
12	17	6.32	0.920	0.1456	6.87
13	7	22.56	0.929	0.0412	24.28
14	2	201.07	0.934	0.0046	215.28
Sums		518.84			562.21

Table 6: Rigidity calculations for $d_{north} = 170'$

STAAD Analysis

Now that the stiffnesses of the V-columns are finalized, they must be combined with the stiffnesses of the braced frames in the E-W direction. To determine the braced frame stiffnesses, each frame is modeled in STAAD, a general purpose structural analysis program. Assumptions must be made that the floor slab at ground level is sufficiently stiff to consider braced, so that both frames are modeled from Level 400 to Level 500 only with pinned supports at their bases. Member lengths and section properties were obtained from the plans, column schedule, and braced frame elevations. A 100 kip load was applied at the top of each frame to accurately estimate nodal displacements. Figures 22 and 23 are diagrams of the STAAD models.

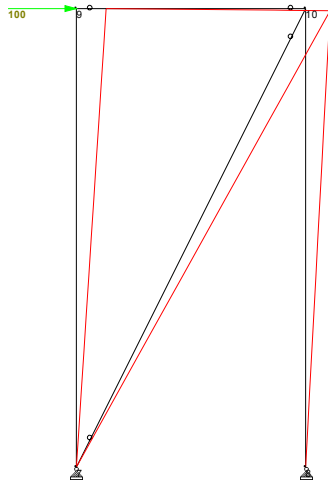


Figure 22: BF1

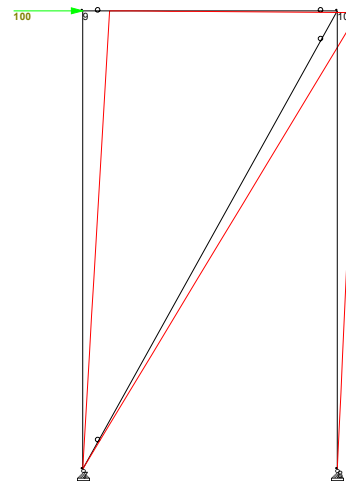


Figure 23: BF4

Both frames were analyzed and their nodal displacements are summarized in Table 7 and Table 8.

BF1

Node	L/C	X (in)	Y (in)
7	1:UNIT WIND	0	0
8	1:UNIT WIND	0	0
9	1:UNIT WIND	0.234	0
10	1:UNIT WIND	0.192	-0.016

Table 7: Node displacements for BF1

Average displacement in the x direction = $(0.234+0.192)/2 = 0.213$

The stiffness (k) of the frame is the applied load over the average displacement, or $(100 \text{ kip})/(0.213 \text{ in.}) = 469.48 \text{ kip/in.}$

BF4

Node	L/C	X (in)	Y (in)
7	1:UNIT WIND	0	0
8	1:UNIT WIND	0	0
9	1:UNIT WIND	0.211	0
10	1:UNIT WIND	0.165	-0.015

Table 8: Node displacements for BF1

Average displacement in x direction = $(0.211+0.165)/2 = 0.188$

The stiffness (k) of the frame is the applied load over the average displacement, or $(100 \text{ kip})/(0.188 \text{ in.}) = 531.91 \text{ kip/in.}$

Combined Results

The stiffnesses for the braced frames are then combined with the stiffnesses of the V columns and inserted into an overall stiffness spreadsheet, similar to those used in the ETABS Analysis (Table 9). The spreadsheet is used to calculate the actual center of rigidity in the x direction for the structure with both V columns and braced frames. It assumes that displacements are equal, which is true when the load acts at the center of rigidity. Torsion will be considered later, along with total building drift. Therefore, the center of rigidity is obtained by dividing the sum of $k*d$ values by the sum of k values in Table 9.

$$\text{Center of Rigidity} = \Sigma(k*d)/\Sigma k = 3587061/2033.09 = 1764 \text{ in.} = 147 \text{ ft.}$$

Adding in the braced frame stiffnesses moves the center of rigidity just north of the geometric center of the building, as shown in Figure 24. Obviously the two BF1 frames in the northern half of the building have a substantial impact on the structure's rigidity.

Support	Node	Reaction	Δ_{unit}	Rigidity (k)	d_{north}	$k*d$
		kips	in.	kips/in.	ft.	kips
1	54	3.89	0.0656	15.25	103	18846
2	51	0.62	0.4102	2.44	130	3803
3	48	0.66	0.3854	2.59	157	4888
4	45	2.37	0.1077	9.28	183	20388
5	42	5.71	0.0447	22.39	210	56433
6	39	10.64	0.0240	41.68	236	118041
7	36	16.78	0.0152	65.77	261	205979
8	33	23.28	0.0110	91.23	286	313099
9	26	9.57	0.0267	37.49	288	129562
10	23	5.00	0.0511	19.58	262	61574
11	20	2.06	0.1239	8.07	235	22757
12	17	1.75	0.1456	6.87	208	17146
13	7	6.20	0.0412	24.28	115	33512
14	2	54.94	0.0046	215.28	73	188584
BF1-N	N/A	119.81	0.0021	469.48	89	501408
BF1-S	N/A	119.81	0.0021	469.48	100	563380
BF4	N/A	135.74	0.0019	531.91	208	1327660
Sums		518.84		2033.09		3587061

Table 9: Overall rigidity calculations

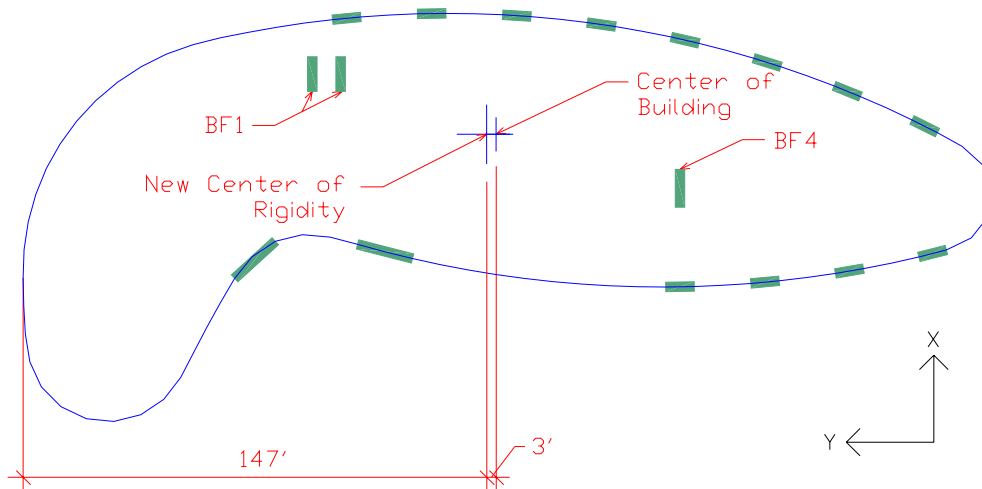


Figure 24: Final center of rigidity location

Now that all stiffness elements are accounted for, the calculated story drift for Level 500 in the x direction can be obtained. This drift is simply the sum of the reactions divided by the sum of the rigidities, or

$$\text{Story Drift} = \Sigma(\text{Reactions})/\Sigma k = 518.84/2033.09 = 0.255 \text{ in.}$$

The allowable drift is once again $L/350$, however the story height from Level 400 to Level 500 is 18', so $\Delta_{all} = (18')*(12 \text{ in./ft.})/350 = 0.432 \text{ in.}$ The actual story drift for Level 500 is less than the allowable story drift and therefore is acceptable.

Torsion

Torsion is a lateral loading situation where the resultant load does not act through the center of rigidity. It must be considered when analyzing the lateral stiffness elements in a building. According to the governing building code, ASCE Standard 7-98 provides the provisions for unbalanced wind loads. Essentially, one half of the building wind load must be reduced by 25 percent to create eccentric loading and therefore torsion. Since it was determined that the structure's center of rigidity does not coincide with the geometric center of the building, the wind must be loaded so that P_w max occurs in the south half of the building. This is summarized below in Figure 25.

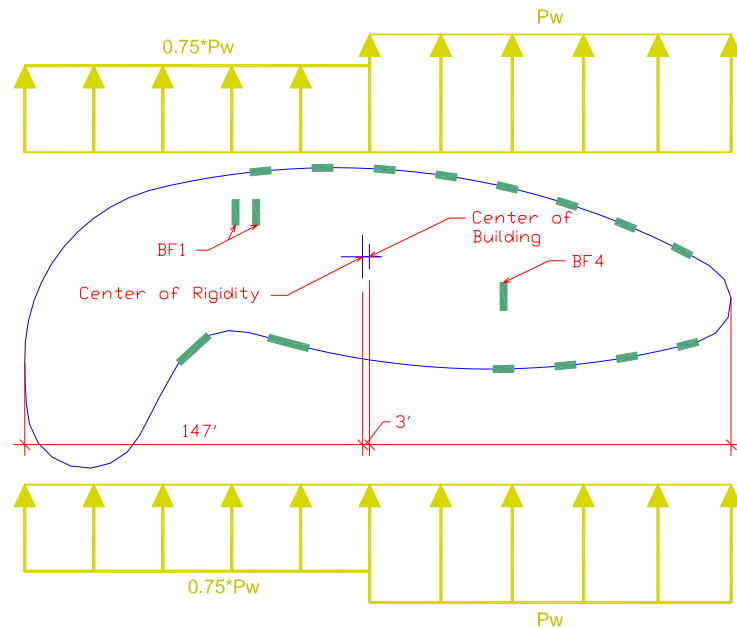


Figure 25: Unbalanced wind loading

The unbalanced moment was found by calculating $P_{unbalanced}$ and e from the loading condition.

$$P_{unbalanced} = P_w * (1/2 * 0.75 + 1/2 * 1.0) = 518.84 * (0.875) = 453.99 \text{ kip}$$

$$e = (0.25 * 0.75 * 0.5 + 0.75 * 1.0 * 0.5) / (0.75 * 0.5 + 1.0 * 0.5) * 300' - \text{Center of Rigidity} \\ = 160.7' - 147' = 13.7' = 165 \text{ in.} = 4.5\% \text{ of the building length}$$

$$M_{unbalanced} = P_{unbalanced} * e = 453.99 * 165 = 74907.5 \text{ in-kip}$$

Using d_{north} , d_i , and final k values, the sum of kd_i^2 terms were calculated in an Excel spreadsheet (Table 10) in order to find $\theta_{torsion}$. The value d_i is the absolute distance from the element to the calculated center of rigidity.

Support	Node	d_{north}	d_i	d_i	Rigidity (k)	$k*d_i$	$k*d_i^2$
		ft.	ft	in	kip/in.	kip	in-kip
1	54	103	44	528	15.25	8050.58	4250706.58
2	51	130	17	204	2.44	497.35	101458.64
3	48	157	10	120	2.59	311.35	37362.16
4	45	183	36	432	9.28	4010.76	1732647.98
5	42	210	63	756	22.39	16929.79	12798923.70
6	39	236	89	1068	41.68	44515.55	47542602.97
7	36	261	114	1368	65.77	89967.70	123075816.89
8	33	286	139	1668	91.23	152170.67	253820676.88
9	26	288	141	1692	37.49	63431.45	107326008.95
10	23	262	115	1380	19.58	27026.89	37297101.64
11	20	235	88	1056	8.07	8521.70	8998916.47
12	17	208	61	732	6.87	5028.52	3680877.91
13	7	115	32	384	24.28	9325.12	3580847.53
14	2	73	74	888	215.28	191167.19	169756469.04
BF1-N	N/A	89	58	696	469.48	326760.56	227425352.11
BF1-S	N/A	100	47	564	469.48	264788.73	149340845.07
BF4	N/A	208	61	732	531.91	389361.70	285012765.96
Sum							1435779380

Table 10: kd_i^2 calculations

Since y-direction stiffnesses were not taken into account in the kd_i^2 terms, an estimate of their rigidity must be made. It can be assumed that the stiffnesses in the x-direction are approximately equal to the stiffnesses in the y-direction. Therefore, the total sum of kd_i^2 is twice the value calculated in Table 10. Rotation due to torsion can be calculated from the small displacement theory torsion equation $\theta_{torsion} = M_{unbalanced} / \sum k_i d_i^2$. This calculation is shown below.

$$\tan(\theta_{torsion}) = \frac{M}{\sum (k_i * d_i^2)} \quad , \quad \tan(\theta_{torsion}) = \frac{74907.5}{2 * 1435779380} \quad , \quad \theta_{torsion} = 0.000026 \text{ rad}$$

The torsional rotation for this case is much lower than what was calculated by ETABS in the original wind load case. This happens for two main reasons, both related to the absence of braced frames in the model. The first is that the center of rigidity for the V columns was much further from the resultant load in the original case. The second is that the total rigidity was much lower in the original case as well, producing more rotation under similar loads.

In any case, $\theta_{torsion}$ produced by a 4.5% eccentricity is extremely small. It will not be much of an issue. At 0.000026 rad, the maximum building drift at the north and south ends for Level 500 will be $\tan(0.000026 \text{ rad}) * 300' / 2 = 0.047 \text{ in.}$ This certainly makes sense, since the elliptical shape of the building and orientation of the V columns and braced frames in relation to the center of rigidity maximizes each element's stiffness potential. As one sees in automobile drive shafts and other related mechanical applications, a round shape naturally resists torsion better than a rectangular shape.

Total Building Drift

Stiffness element forces in the x direction as a result of torsion must be calculated to find the total building drift. F_{torsion} values are calculated by dividing the individual $k_i d_i$ values by twice the sum of $k_i d_i^2$ in Table 10 and multiplying by the unbalanced moment. F_{direct} values are the reactions obtained from the direct load story drifts in Table 9. Displacement from Level 400-500 at each support is found by dividing F_{total} by the rigidity. Displacements from Levels 500-900 are found from Table 2. Finally, the total drift is simply the sum of the story drifts from Levels 400-500 and 500-900. Table 11 contains all of these values.

Support	Node	F_{torsion}	F_{direct}	F_{total}	Rigidity (k)	$\Delta_{400-500}$	$\Delta_{500-900}$	Δ_{total}
		kip	kip	kip	kips/in.	in.	in.	in.
1	54	0.21	3.89	4.10	15.25	0.269	0.170	0.439
2	51	0.01	0.62	0.64	2.44	0.261	0.178	0.439
3	48	0.01	0.66	0.67	2.59	0.258	0.187	0.445
4	45	0.10	2.37	2.47	9.28	0.266	0.195	0.461
5	42	0.44	5.71	6.16	22.39	0.275	0.203	0.478
6	39	1.16	10.64	11.80	41.68	0.283	0.211	0.494
7	36	2.35	16.78	19.13	65.77	0.291	0.219	0.510
8	33	3.97	23.28	27.25	91.23	0.299	0.227	0.526
9	26	1.65	9.57	11.22	37.49	0.299	0.225	0.524
10	23	0.71	5.00	5.70	19.58	0.291	0.217	0.508
11	20	0.22	2.06	2.28	8.07	0.283	0.208	0.491
12	17	0.13	1.75	1.88	6.87	0.274	0.200	0.474
13	7	0.24	6.20	6.44	24.28	0.265	0.176	0.441
14	2	4.99	54.94	59.93	215.28	0.278	0.161	0.439
							Max	0.526

Table 11: Maximum building drift at support nodes

The allowable drift for the total building height as found in the specifications is $L/500$. Total building height is $18' + 4 \times 13.5' = 72'$, therefore $\Delta_{\text{all}} = (72')/500 = 1.728$ in. The maximum building drift from Table 11 is 0.526 in., well within the allowable drift. Maximum drift occurs near node 33, at the southern tip of the building. This result makes sense, since the wind forces acting on both the diagrid structure (refer to Figure 16) and the v-columns cause greater deflection at the southern end of the building.

Overtuning

To determine overturning reactions the unfactored wind and dead loads are combined and applied in the ETABS model used for lateral drift. Two-thirds of the dead load of each level as calculated in Appendix A is modeled in order to conservatively estimate the minimum dead load. This weight is applied as a uniform area load on every floor, including Level 900, the roof. The weights used in the overturning analysis are shown below in Table 12.

Level	Superimposed (kip)	Superstructure (kip)	Total (kips)	Area ft ²	Uniform Load psf
900 (Roof)	1973	368	2341	23500	100
800	2084	438	2522	23500	107
700	2100	438	2538	23500	108
600	2361	438	2800	23500	119
500	2209	390	2600	23500	111
Sums			12800	117500	

Table 12: Dead Loads used in overturning analysis

The analysis was performed and the resulting reactions are summarized in Table 13.

Support	FZ (2/3 D)	Support	FZ (2/3 D)	Support	FZ (2/3 D)
1	511	7	323	13	803
2	323	8	388	14	751
3	319	9	435	15	825
4	318	10	319	16	480
5	316	11	319	17	1170
6	316	12	619	Sum (1-17)	2103

Table 13: Overturning reactions

Since all the FZ values are positive, there are no net uplift forces acting at the supports. Therefore, supporting columns and piers do not experience tensile forces, which is significant in the subsequent foundation design. These results make sense because the relatively low building height does not provide enough wind force overturning moment to overcome the wide base of the diagrid frame.

Member Checks

In order to keep member checking workload reasonable, only two types of lateral force resisting members are evaluated. The braced frames are critical elements in the lateral system and will be analyzed. Also, the unique structural concept of the diagrid will be looked at.

Braced Frames

First, F_{torsion} values are found using the equations in the Total Building Drift section. They are combined with the F_{direct} from Table 9 to obtain F_{total} , summarized in Table 14 below.

Support	Node	F_{torsion}	F_{direct}	F_{total}
		kip	kip	kip
BF1-N	N/A	8.52	119.81	128.33
BF1-S	N/A	6.91	119.81	126.72
BF4	N/A	10.16	135.74	145.90

Table 14: Total frame forces

The F_{total} forces are inputted into STAAD using the 1.6 wind factor from load case 4. BF1-N was used to model both BF1 frames because it has a higher F_{total} . Axial forces for the diagonals were taken from the STAAD output (Appendix E.1 and Appendix E.2). Unbraced lengths were determined from frame geometry. Since the members are part of a braced frame system, the k factor was assumed to be 1.0. Using Table 4-2 in the LRFD manual (3rd edition), the least weight beams for three common column sizes were found. Results are summarized below in Table 15.

Frame Member	Axial force	Lb	K	KLy	Least Weight Beam		
	kip	ft		ft	W10x	W12x	W14x
BF1 Diagonal	460.80	20.1	1.0	20.1	77	65*	74
BF4 Diagonal	482.40	20.6	1.0	20.6	77	65*	82

*non-compact

Table 15: Braced frame member sizing

The actual diagonal sizes are both W14x90. The differences between this member and the possible least weight members above can be attributed to a variety of factors. Seismic loads, which were not considered in this check, could be the controlling loads on the braced frames. Other load cases might be applicable as well. The addition of dead loads to the model would increase P-delta effects and add compressive load to the diagonal. Connections to the rest of the frame might be more feasible with a W14 as opposed to a smaller depth. Also, inaccuracy of the model and its resulting loads could contribute to the size discrepancy. However, these possible members are certainly in the ballpark of the actual W14x90 diagonals.

Diagrid Members

To accurately size the diagrid members gravity loads must be included in the ETABS analysis. A simplified procedure is used to determine the correct gravity loads acting on the diagrid. We will look only at the western office bays, since they are the most representative areas of the building. They are modeled with a 15' tributary area depth wrapping around the entire building (Figure 26). The rest of the load in the bays is considered to go to interior columns. This is certainly not true throughout the entire building, however, it is a reasonable approximation.

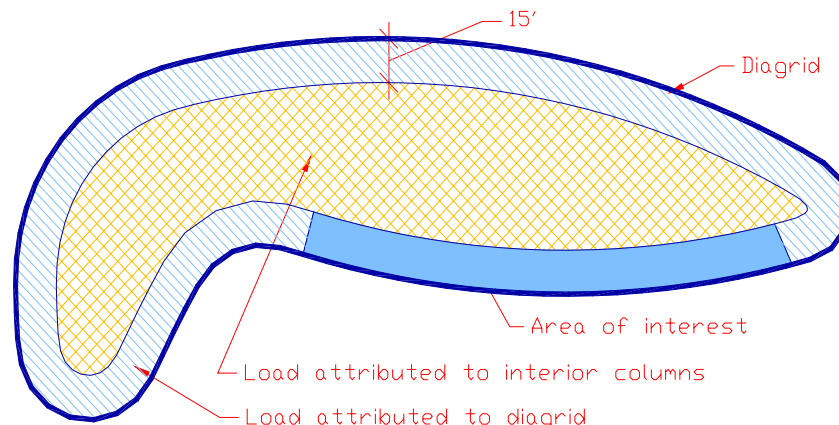


Figure 26: Simplified loading tributary depth

The width of the tributary area to each node on the diagrid is the width of a diagrid bay, or 9' o.c. The tributary area at each level is therefore 9'x15' = 135 ft². This area is attributed to Levels 500-900, with the top area being the roof, as illustrated in Figure 27.

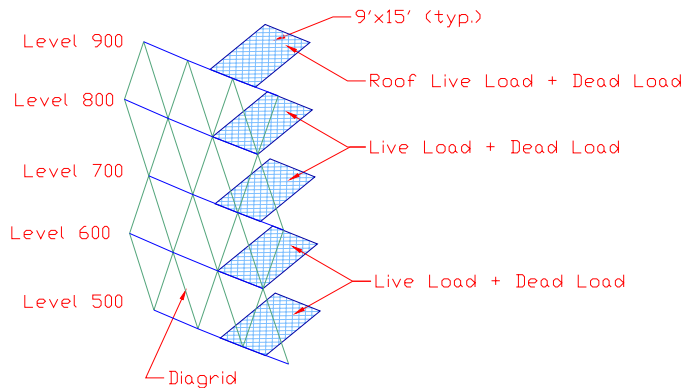


Figure 27: Simplified loading tributary width

Dead, live, and roof snow loads are taken from Appendix A. Dead loads are summarized in Table 16. Though ETABS does have Live Load Reduction capabilities, they are not applicable to the type of simplified model we are working with. Therefore, Live Load Reductions are included with snow loads in Table 17 according to ASCE 7-98. It has been assumed that the roof snow load controls over the roof live and roof rain loads. Because of the unusual geometry of the diagrid, the actual area that directs live load toward each node is in fact higher than the simplified tributary area assumed above. This means that the numbers below are likely conservative. This is illustrated in Figure 28.

	Area ft ²	Roof Dead psf	Area ft ²	Office Dead psf	Total Dead kip
Level 900	135	95	0	96	12.8
Level 800	135	95	135	96	25.8
Level 700	135	95	270	96	38.7
Level 600	135	95	405	96	51.7
Level 500	135	95	540	96	64.7

Table 16: Diagrid dead loads

	Area ft ²	Snow psf	Total Snow kip	Area ft ²	Office Live psf	KII	LLR	Reduced LL psf	Total Live kip
Level 900	135	30	4.1	0	50	4	1	50.0	0.0
Level 800	135	30	4.1	135	50	4	0.895	44.8	6.0
Level 700	135	30	4.1	270	50	4	0.706	35.3	9.5
Level 600	135	30	4.1	405	50	4	0.623	31.1	12.6
Level 500	135	30	4.1	540	50	4	0.573	28.6	15.5

Table 17: Diagrid snow and live loads

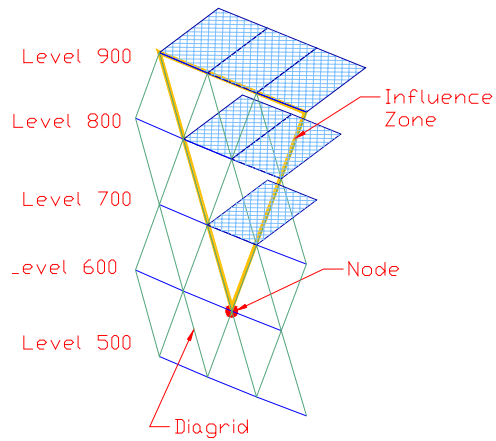


Figure 28: Diagrid load influence zone

The dead, live, and snow loads were then inputted into ETABS as point loads at each node. Appropriate load combination factors, in accordance with the Ohio Basic Building Code, were evaluated. Refer to the Load Cases section for those combinations.

Once the model was analyzed in ETABS, axial and moment forces were obtained for the entire diagrid structure. Graphical outputs shown in Figure 29 (axial force) and Figure 30 (moments) help locate areas of high stress. Two regions of members were selected to be further investigated, based on the sectional properties of the members and their proximity to the office bays for which the loading was modeled.

The green region, on the western side of the building, has the following properties, as found on the structural drawings:

- Upper Diagrid (top two floors) – Horizontals W14x82, Diagonals W12x53
- Lower Diagrid (bottom two floors) – Horizontals W14x82, Diagonals W12x87

The purple region, on the southern tip of the building, has different properties:

- Upper Diagrid (top two floors) – Horizontals W14x53, Diagonals W12x35
- Lower Diagrid (bottom two floors) – Horizontals W14x53, Diagonals W12x50

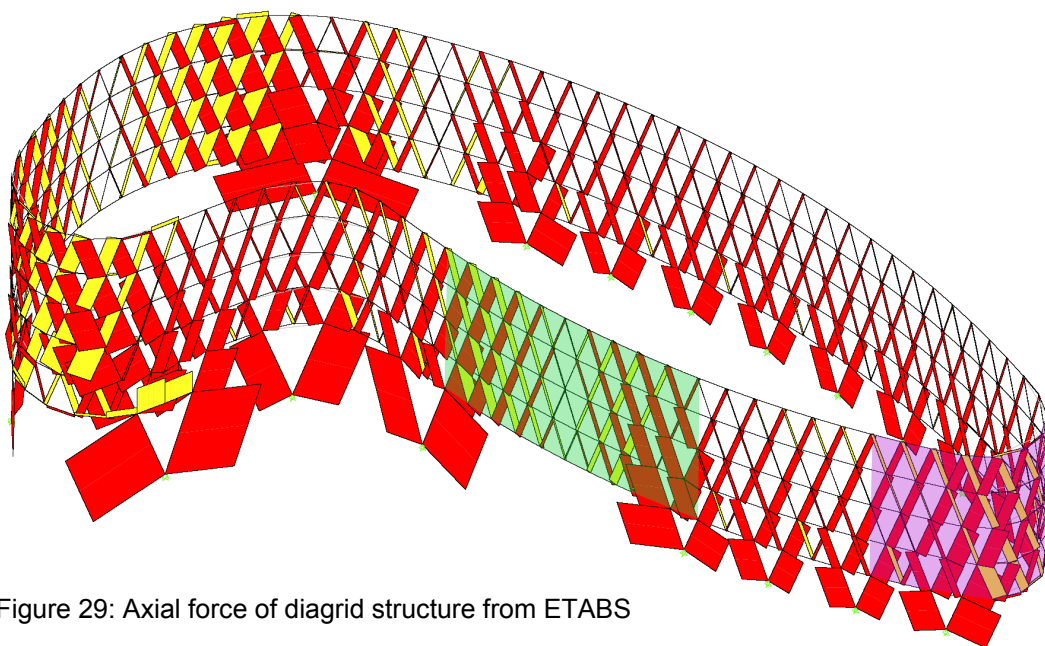


Figure 29: Axial force of diagrid structure from ETABS

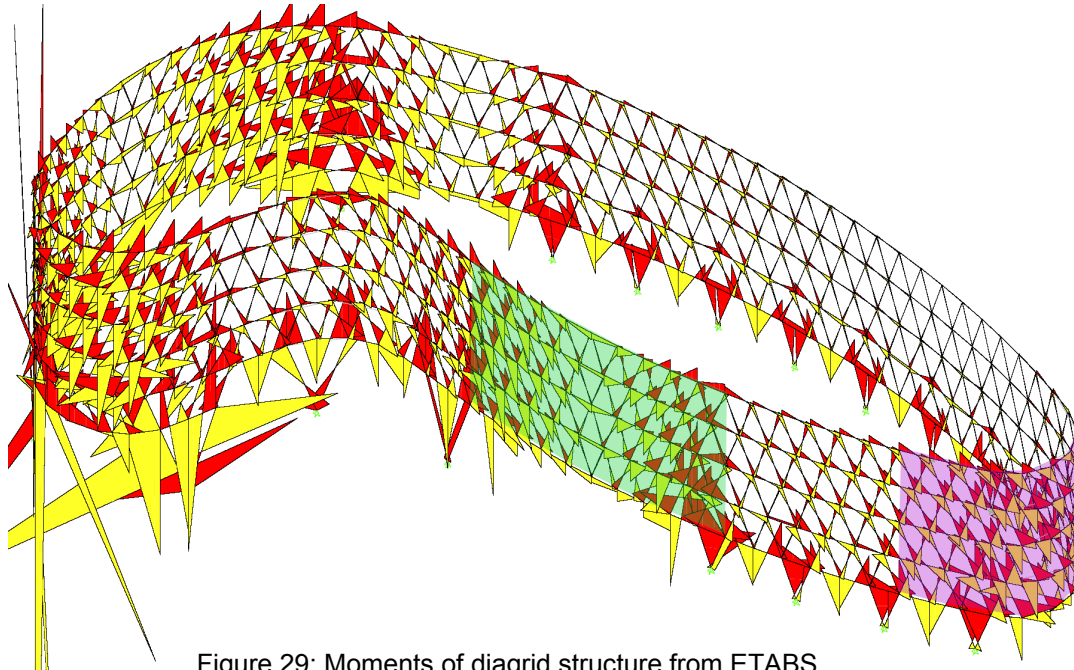


Figure 29: Moments of diagrid structure from ETABS

Due to the high number of members to be analyzed, an Excel spreadsheet was developed which calculates the interaction equation utilization factor. The maximum factored forces for required strength are taken from the ETABS output, while the calculations for nominal strength are calculated per LRFD specification, shown below in Table 18. Unbraced lengths were calculated from diagrid geometry and ΦP_n (compression) was obtained using Table 4-2 in the LRFD manual (3rd edition).

Steel Properties			Tension Capacity		Compression Capacity				
Fy	50			Ag	ΦP_n (tens.)	Lx = Ly	κ	KLx = KLy	ΦP_n (comp.)
Φt	0.9			in	kip	ft		ft	kip
Φb	0.9								
Green	Horizontal	W14x82	24.0	1080	9.0	1.0	9.0	888	
	Diagonal	W12x87	25.6	1152	14.2	1.0	14.2	870	
Purple	Horizontal	W14x53	15.6	702	9.0	1.0	9.0	526	
	Diagonal	W12x50	14.6	657	14.2	1.0	14.2	360	

			Moment Capacity			
			Zx	$\Phi M_n x$	Zy	$\Phi M_n y$
			in ³	in-kip	in ³	in-kip
Green	Horizontal	W14x82	139	6255	44.8	2016
	Diagonal	W12x87	132	5940	60.4	2718
Purple	Horizontal	W14x53	87.1	3920	22.0	990
	Diagonal	W12x50	71.9	3236	21.3	959

Table 18: Nominal strength calculations

First page samples of the spreadsheets are included in Appendix F. Full results are not included because they are unnecessary and repetitive, but are available upon request. The number of members controlled by each load case is shown below in Table 19. As you can see, Case 4, which includes wind loading, controls in more than 75% of the members in the regions analyzed.

	Green		Purple		Total
	Horizontal	Diagonal	Horizontal	Diagonal	
Case 1	0	0	0	0	0
Case 2	6	24	13	14	57
Case 3	0	0	0	1	1
Case 4	46	64	29	57	196

Table 19: Controlling cases summary

If a diagrid member is sufficient to carry the design loads its utilization factor must be less than 1.0. For each type of member in both regions, the maximum utilization factor was obtained from the spreadsheets. These factors are summarized below in Table 20.

			Max. Utilization Factor	Load Case
Green	Horizontal	W14x82	0.324	Case 4
	Diagonal	W12x87	0.586	Case 4
Purple	Horizontal	W14x53	0.440	Case 4
	Diagonal	W12x50	0.861	Case 4

Table 20: Maximum Utilization Factor Summary

Since the utilization factors are all less than 1.0, it can be concluded that the diagrid members for the two regions considered are adequate to carry their imposed loads. However, it must be noted that the utilization factor for the horizontals in both regions are well under 0.5, meaning less than half of their allowed strength is being used under worst case conditions. Though this may seem like severe under-design, several important factors may contribute these results.

- First and foremost, the diagrid has been designed to be as consistent as possible along its length. It is economical to use similar member sections where required strengths are similar, especially when ease of construction is considered. In order for all members to meet those strengths many of the members in low stress areas will be underutilized.
- Since only a portion of the diagrid was analyzed, it is quite possible that in the areas of higher stress around the northwest tip (refer to Figures 29 and 30) the utilization factor approaches 1.0.
- Gravity loading was made by an approximate method. More accurate tributary areas would have to be evaluated to obtain true loading conditions.
- Deflection, seismic, and redundancy issues were not taken into consideration.

- The unconventional shape of a structure such as this leaves a significant amount of uncertainty in its anticipated behavior. It is ultimately up to the experience of the engineer to increase member sizes if there is any doubt in the structure's strength and serviceability performance.

Conclusions

The University of Cincinnati Athletic Center performs quite well under lateral loading situations. Seven distinct analyses were performed, and in all cases the designed structure met or exceeded allowable values. Specific conclusions for each analysis type are explained below.

Diagrid Story Drift

The high rigidity and redundancy of the diagrid and its diaphragms provide an excellent distribution of wind load from the exterior faces down to the ground level supports. Drifts calculated using ETABS are well within the specified L/350 limits. In fact, actual story drifts are always less than 1/4 the allowable story drift.

Ground Floor Story Drift

The three braced frames account for most of the lateral resistance in the E-W direction. Excel spreadsheets show that calculated drifts are well under the specified L/350 limits. Actual story drifts are less than 1/3 the allowable story drift.

Torsion

Building rotation due to unbalanced wind loads is extremely small. The elliptical shape of building is well-suited to resisting torsional forces.

Total Building Drift

Even with torsion considered the maximum total drift is less than 1/3 the allowable drift.

Overtipping

No uplift forces were obtained with a conservative dead load approach. The relatively low building height does not provide enough wind force overturning moment to overcome the wide base of the diagrid frame

Braced Frame Check

The actual member sizes for the braced frame diagonals are slightly larger than calculated member sizes. The members are not, however, overdesigned, but could be resisting forces which were not accounted for in the model.

Diagrid Member Check

From ETABS output and Excel charts, the maximum utilization factor of the evaluated members = 0.861. Since this is less than 1.0 the members are adequate to carry their loads. Some members are potentially overdesigned, but there are many valid reasons for doing so.

Gravity Loads

Gravity loads consist of the superstructure dead load, the superimposed dead load, and live loading.

Superstructure load – A computer analysis program was used by the structural engineer to determine the self weight of the superstructure. For this report the self weight was estimated using a simplified procedure. The theory behind the procedure is found in Appendix A.2, while the load calculations are tabulated in Appendix A.3.

Superimposed load – Loading diagrams on the drawings were used to compile total superimposed loads for each floor. Appendix A.4 shows the dead load for each type of occupancy in the “Total Dead” column. Appendix A.5 tabulates the total load for each floor. Dead Loads are summarized below.

Level	Superimposed (kip)	Superstructure (kip)	Total (kips)
Roof	1973	368	2341
800	2084	438	2522
700	2100	438	2538
600	2361	438	2800
500	2209	390	2600
400 (ground)	5026	460	5486

Live load – Loading diagrams on the drawings were used to compile live loads for each floor. Appendix A.4 shows the live load for each type of occupancy in the “Live Load” column. Snow loads were assumed to be 30psf with 50psf drifts as indicated on the drawings.

SUPERSTRUCTURE

Job Title UCAL CONST. DEAD LOADS THEORY

Member-Location

Drg. Ref.

Made by BTG Date 10.7.03

Chd.

SUPERIMPOSED LOADS

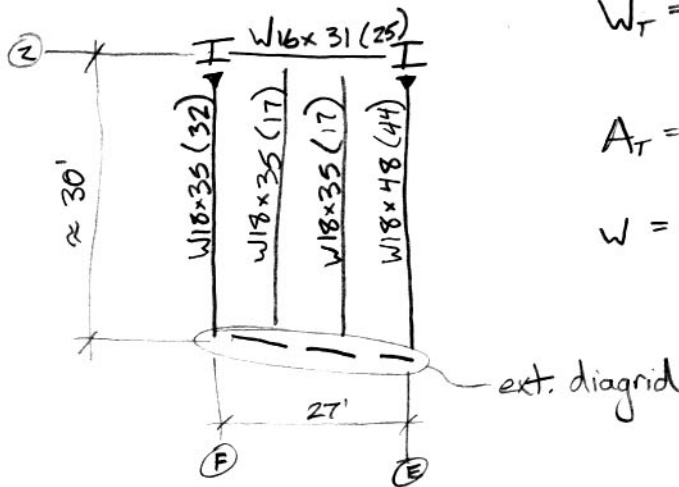
SEE Excel Spreadsheet, taken from drawings

CONST. LOADS

FLOOR FRAMING

Find a typical bay:

FLOOR 4 (700)



$$W_T = 31 \cdot 27 + 35 \cdot 30 \cdot 3 + 48 \cdot 30 + (25 + 32 + 2 \cdot 17 + 44) \cdot 10 = 6780 \text{ lbs.}$$

$$A_T = 30 \cdot 27 = 816 \text{ sf.}$$

$$w = \frac{W_T}{A_T} = \frac{6780}{816} = 8.37 \text{ psf} \Rightarrow 10 \text{ psf (conservative)}$$

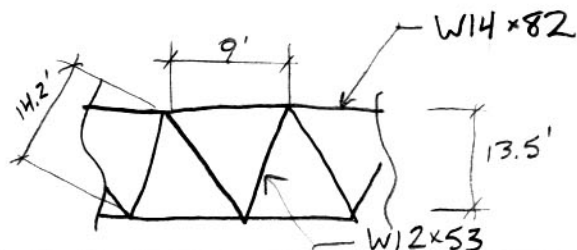
COLUMNS

	# of cols	Typ weight (plf)	Height	Wt/Floor
not necessarily } LEVELS 100-300	44 cols	170	15'	112.2 ^k
LEVEL 300-400	63 cols	170	14'	149.9 ^k
LEVEL 400-500	21 cols	120	18'	45.4 ^k
LEVELS 500-Roof	17 cols	60	13.5'	13.8 ^k

Summarized in Excel

ENCLOSURE

Typ Frame size + geometry:
(from dwgs.)



--	--	--

Member-Location

Job Title Drg. Ref.

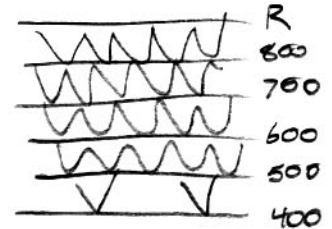
Made by Date Chd.

ENCLOSURE (CONT'D)

Perimeter found by CAD = 760'

Horiz. members: $82 \cdot 760' = 62.3^k / \text{level}$

Diag. members: $53 \cdot 14.2' \cdot \frac{760'}{4.5} = 127.1^k / \text{level}$



CALCS IN EXCEL

Appendix A.3 - Gravity Load Calculations

Superstructure Dead Load

Level	Floor Framing				Columns						Enclosure			
	Dist. Load (psf)	Area (ft ²)	Weight/floor (kips)		# of cols.	Typ. weight (plf)	Story Ht. (ft)	Wt./floor (kips)	Trib. Wt. (kips)	Horiz. Mem. (kips)	Diag. Mem. (kips)	Trib. Wt. (kips)	Total	
Roof	10	23500	235		17	60	13.5	13.8	6.9	62.3	127.1	63.6	367.7	
800	10	23500	235		17	60	13.5	13.8	13.8	62.3	127.1	127.1	438.2	
700	10	23500	235		17	60	13.5	13.8	13.8	62.3	127.1	127.1	438.2	
600	10	23500	235		17	60	13.5	13.8	13.8	62.3	127.1	127.1	438.2	
500	10	23500	235		17	60	13.5	13.8	13.8	62.3	127.1	63.6	390.4	
400	10	37500	375		21	120	18	45.4	22.7	62.3			460.0	

Appendix A.4 - Gravity Load Calculations

Superimposed Load Types

	Area Occupancy	Floor Finish (psf)	Floor Slab (psf)	Ceiling/Services (psf)	Partitions (psf)	Additional (psf)	Total Dead (psf)	Live Load (psf)	Total Unfactored (psf)
1	High Roof		60	10			70	30	100
2	Office		66	10	20		96	50	146
3	Multi-purpose club		66	10			76	100	176
4	Stair					30	30	100	130
5	Atrium/Corridor	25	66	10			101	100	201
6	Mechanical room		66	10		50	126	125	251
7	Computer lab	25	66	10			101	100	201
8	Fixed seating		110	10		10	130	60	190
9	Stage	25	66	10			101	100	201
10	Lobby/General assembly	25	66	10			101	100	201
11	Locker room	25		10	20		55	100	155
12	Work area	25	65	10	20		120	100	220
13	Showers/Rest room	25	66	10			101	60	161
14	Storage	25	66	10			101	125	226
15	Laundry	25		10			35	150	185
16	Ramp	25	66				91	100	191
17	Elevator machine room		66				66	250	316
18	Meeting room		66	10			76	60	136
19	Treatment area	25	66	10	20		121	100	221
20	Video room	25	66	10	20		121	100	221
21	Hydrotherapy	25	66	10			101	400	501
22	Loading dock	30	66	10			106	100	206
23	Ambulance parking	30	79	10			119	100	219
24	Walkway roof	13	5				18	30	48
25	Theater control room	25	66	10	20		121	100	221
26	Trash compactor		66	10			76	350	426
27	Roof	25	60	10			95	60	155
28	Exterior truck loading	90	79	10			179	100	279
29	Exterior non-truck loading	90	66	10			166	100	266

Appendix A.5 - Gravity Load Calculations

10/8/2003

University of Cincinnati Athletic Center
Brian Genduso

Superimposed Dead Load Calculations

Type	100		200		300		400		500		600		700		800		Roof		
	Area (ft ²)	Total (kip)	Area (ft ²)	Total (kip)	Area (ft ²)	Total (kip)	Area (ft ²)	Total (kip)	Area (ft ²)	Total (kip)	Area (ft ²)	Total (kip)	Area (ft ²)	Total (kip)	Area (ft ²)	Total (kip)	Area (ft ²)	Total (kip)	
1																			
2			2224	214	997	96	3586	344	7583	728	10249	984	9973	957	10038	964	10382	727	
3													4234	322	4772	363			
4			483	14	669	20	1046	31	1615	48	1428	43	1694	51	1655	50			
5			3750	379	3598	363			6170	623	5887	595	6106	617	6058	612			
6			1558	196	10932	1377					5472	689							
7									2228	225									
8							2307	300	2485	323									
9							803	81					544	55					
10							8907	900											
11	17259	949																	
12																			
13																			
14			641	65			2017	204	1053	106	501	51	969	98	955	96			
15	4393	154																	
16																			
17	358	24																	
18			8510	647	548	42													
19			3529	427	1749	212													
20																			
21			943	95															
22					2556	271													
23					1033	123													
24																			
25																			
26					451	34			1282	155									
27																			
28					5050	904	4723	845									13119	1246	
29							13982	2321											
Sums	22010	1127	21638	2037	28470	3523	37371	5026	22416	2209	23537	2361	23520	2100	23478	2084	23501	1973	

--	--

Member-Location _____

Job Title UCAL Wind Calcs.

Drg. Ref. _____

ASCE 7-98 Ch. 6

Made by BJG Date 10.6.03 Chd. _____

IS THE BUILDING RIGID?

From ASCE 7-98, 9.5.3.3 $T_a = C_T \cdot h_n^{\frac{3}{4}}$ (period)

$C_T = .02$ (for braced w/ moment frames)

$h_n = 72'$ (from level 400)

$T_a = .02 \cdot 72^{\frac{3}{4}} = .49$ s

$f = \frac{1}{T_a} = \frac{1}{.49} = 2.02 \frac{\text{cyc}}{\text{s}}$ (frequency)

$f > 1 \text{ Hz} \therefore$ building is rigid

Find pressures

$P_w = q_z \cdot G \cdot C_p$ (rigid)

$P_l = q_h \cdot G \cdot C_p$

$q_z = .00256 K_z \cdot K_{zt} \cdot K_d \cdot V^2 \cdot I$

$K_z = .57$ 0-15ft (Exposure B, Case 2 - Table 6-5)

.62	20'
.66	25'
.70	30'
.76	40'
.81	50'
.85	60'
.89	70'
.93	80'

from Figure 6-2 using geotech data

$K_{zt} = (1 + K_1 K_2 K_3)^2 = (1 + .6 \cdot 1.0 \cdot .14)^2 = 1.18$

$K_d = .85$ (Table 6-6)

$V = 90$ mph (Figure 6-1)

$I = 1.15$ (Table 6-1, Category III)

$G = .85$ (assumed)

$C_p = .8$ (windward)

$-.2$ ($L/B \approx \frac{700}{280} = 2.5$, leeward N-S)

$-.5$ ($L/B \approx \frac{170}{300} = .4$, leeward E-W)

Job Title UCAC Wind Calcs

Drg. Ref.

ASCE 7-98

Made by BJG Date 10.6.03

Chd.

$$q_h = \frac{72-70}{80-70} (.93-.89)(q_z) + (q_z) \cdot .89$$

$$q_z = .00256 \cdot 1.18 \cdot .85 \cdot 90^2 \cdot 1.15 \cdot K_{zt} = 23.9 K_z$$

$$q_h = 21.5 \text{ psf}$$

$$p_w = 23.9 \cdot K_z \cdot .85 \cdot .8 = 16.3 \cdot K_z \text{ (Windward, N-S or E-W)}$$

$$p_e = 21.5 \cdot .85 \cdot (-.2) = -3.7 \text{ psf (Leeward, N-S)}$$

$$p_e = 21.5 \cdot .85 \cdot (-.5) = -9.1 \text{ psf (Leeward, E-W)}$$

Calculations

Done in Excel

Appendix B.1 - Wind and Seismic Load Calculations

University of Cincinnati Athletic Center
 Brian Genduso

10/8/2003

N-S Direction

Coefficients	
Windward	16.3
Leeward	-3.7

Height (ft)	Kz	Windward (psf)	Leeward (psf)	Total MWFRS (psf)
0-15	0.57	9.3	-3.7	13.0
15-20	0.62	10.1	-3.7	13.8
20-25	0.66	10.8	-3.7	14.5
25-30	0.70	11.4	-3.7	15.1
30-40	0.76	12.4	-3.7	16.1
40-50	0.81	13.2	-3.7	16.9
50-60	0.85	13.9	-3.7	17.6
60-70	0.89	14.5	-3.7	18.2
70-80	0.93	15.2	-3.7	18.9

E-W Direction

Coefficients	
Windward	16.3
Leeward	-9.1

Height (ft)	Kz	Windward (psf)	Leeward (psf)	Total MWFRS (psf)
0-15	0.57	9.3	-9.1	18.4
15-20	0.62	10.1	-9.1	19.2
20-25	0.66	10.8	-9.1	19.9
25-30	0.70	11.4	-9.1	20.5
30-40	0.76	12.4	-9.1	21.5
40-50	0.81	13.2	-9.1	22.3
50-60	0.85	13.9	-9.1	23.0
60-70	0.89	14.5	-9.1	23.6
70-80	0.93	15.2	-9.1	24.3

Appendix B.3 - Wind and Seismic Load Calculations

N-S Direction

Building height (ft)	72
Building trib width (ft)	120

Level	Story ht. (ft)	Trib ht. (ft)	Total ht. (ft)	P 1 (psf)	H 1 (ft)	P 2 (psf)	H 2 (ft)	P 3 (psf)	H 3 (ft)	Story Dist. Load (plf)	Cum. Dist. Load (plf)	Story Shear (kips)	Cum. Shear (kips)
Roof	13.5	6.75	65.25	18.2	4.75	18.9	2			124	124	14.9	14.9
800	13.5	13.5	51.75	17.6	8.25	18.2	5.25			241	365	28.9	43.8
700	13.5	13.5	38.25	16.1	1.75	16.9	10	17.6	1.75	228	593	27.4	71.2
600	13.5	13.5	24.75	14.5	0.25	15.1	5	16.1	8.25	212	805	25.4	96.6
500	18	15.75	9	13	6	13.8	5	14.5	4.75	216	1021	25.9	122.5
400 (ground)		9		13	9					N/A	N/A	N/A	122.5

E-W Direction

Building height (ft)	72
Building trib width (ft)	300

Level	Story ht. (ft)	Trib ht. (ft)	Total ht. (ft)	P 1 (psf)	H 1 (ft)	P 2 (psf)	H 2 (ft)	P 3 (psf)	H 3 (ft)	Story Dist. Load (plf)	Cum. Dist. Load (plf)	Story Shear (kips)	Cum. Shear (kips)
Roof	13.5	6.75	65.25	23.6	4.75	24.3	2			161	161	48.2	48.2
800	13.5	13.5	51.75	23	8.25	23.6	5.25			314	474	94.1	142.3
700	13.5	13.5	38.25	21.5	1.75	22.3	10	23	1.75	301	775	90.3	232.6
600	13.5	13.5	24.75	19.9	0.25	20.5	5	21.5	8.25	285	1060	85.5	318.0
500	18	15.75	9	18.4	6	19.2	5	19.9	4.75	301	1361	90.3	408.3
400 (ground)		9		18.4	9					N/A	N/A	N/A	408.3

Job Title UCAC Seismic Calcs

Drg. Ref.

ASCE 7-98 Ch. 9

Made by BTG

Date 10.7.03

Chd.

Determine Seismic Design Category

From Wind Analysis, Table 1-1, Occupancy Category = III

 \therefore Seismic Use Group = II (Table 9.1.3)Site classification

From Basis of Design report, in conjunction w/ the geotech report from H.C. Nutting Co., Site class. = B

(rock w/ $2500 \frac{\text{lb}}{\text{ft}^3} \leq \gamma_s \leq 5000$)Spectral Response Accelerations

$$S_s = .20 \quad (\text{from Figure 9.4.1.1 (a)})$$

$$S_1 = .09 \quad (\text{from Figure 9.4.1.1 (b)})$$

$$F_a = 1.0 \quad (\text{Table 9.4.1.2.4a})$$

$$F_v = 1.0 \quad (\text{Table 9.4.1.2.4b})$$

$$S_{MS} = F_a \cdot S_s = 1.0 \cdot .2 = .20 g \quad \leftarrow \text{gravitational constant}$$

$$S_{M1} = F_v \cdot S_1 = 1.0 \cdot .09 = .09 g$$

$$S_{DS} = \frac{2}{3} S_{MS} = \frac{2}{3} \cdot .2 = .133 g$$

$$S_{D1} = \frac{2}{3} S_{M1} = \frac{2}{3} \cdot .09 = .06 g$$

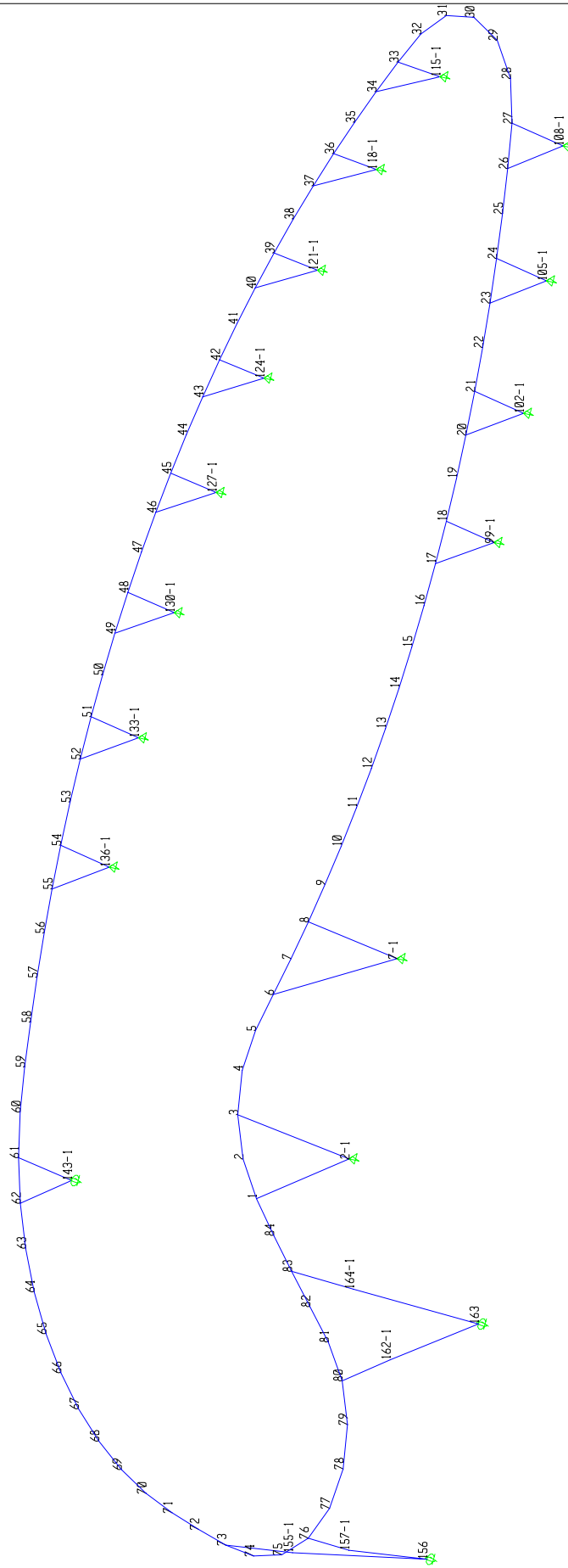
From Table 9.4.2.1a, SDC = A \therefore SDC = A

From Table 9.4.2.1b, SDC = A

Section 9.5.2.5.1 specifies that a building in SDC = A can be designed using $F_x = .01 w_x$

Excel used to calculate story shear

Appendix C - Node Numbering System



Appendix D.1 - ETABS Analysis Results

ETABS v8.2.6 File: ETABS MODEL 2 (WITH RIGID DIAPHRAGM) Kip-in Units PAGE 1
November 7, 2003 18:11

AE 431W
3D ETABS Model

P O I N T D I S P L A C E M E N T S

STORY	POINT	LOAD	UX	UY	UZ	RX	RY	RZ
STORY1	1	WWIND	1.4252	0.1160	0.2513	-0.00061	0.00222	-0.00026
STORY1	2	WWIND	1.4076	0.0941	0.0247	0.00085	0.00159	-0.00026
STORY1	3	WWIND	1.3844	0.0787	-0.1685	-0.00077	0.00370	-0.00026
STORY1	4	WWIND	1.3574	0.0720	-0.1014	-0.00040	-0.00029	-0.00026
STORY1	5	WWIND	1.3295	0.0745	-0.0905	0.00022	0.00021	-0.00026
STORY1	6	WWIND	1.3021	0.0818	-0.1106	0.00022	0.00321	-0.00026
STORY1	7	WWIND	1.2747	0.0893	-0.0122	-0.00062	0.00081	-0.00026
STORY1	8	WWIND	1.2471	0.0961	0.0924	0.00021	0.00326	-0.00026
STORY1	9	WWIND	1.2194	0.1022	0.0485	0.00041	0.00042	-0.00026
STORY1	10	WWIND	1.1915	0.1075	0.0379	0.00009	0.00045	-0.00026
STORY1	11	WWIND	1.1635	0.1121	0.0336	0.00009	0.00045	-0.00026
STORY1	12	WWIND	1.1353	0.1161	0.0292	0.00009	0.00046	-0.00026
STORY1	13	WWIND	1.1070	0.1193	0.0241	0.00008	0.00047	-0.00026
STORY1	14	WWIND	1.0787	0.1217	0.0181	0.00008	0.00049	-0.00026
STORY1	15	WWIND	1.0504	0.1234	0.0111	0.00007	0.00050	-0.00026
STORY1	16	WWIND	1.0220	0.1245	0.0001	0.00023	0.00068	-0.00026
STORY1	17	WWIND	0.9935	0.1247	-0.0244	-0.00027	0.00434	-0.00026
STORY1	18	WWIND	0.9651	0.1243	0.0201	-0.00039	0.00402	-0.00026
STORY1	19	WWIND	0.9367	0.1231	0.0043	0.00018	0.00088	-0.00026
STORY1	20	WWIND	0.9084	0.1212	-0.0110	-0.00052	0.00504	-0.00026
STORY1	21	WWIND	0.8801	0.1185	0.0066	-0.00062	0.00505	-0.00026
STORY1	22	WWIND	0.8519	0.1151	0.0055	-0.00009	0.00090	-0.00026
STORY1	23	WWIND	0.8237	0.1110	0.0056	-0.00063	0.00457	-0.00026
STORY1	24	WWIND	0.7957	0.1062	-0.0088	-0.00072	0.00454	-0.00026
STORY1	25	WWIND	0.7678	0.1007	0.0071	-0.00034	0.00083	-0.00026
STORY1	26	WWIND	0.7401	0.0944	0.0211	-0.00068	0.00408	-0.00026
STORY1	27	WWIND	0.7126	0.0874	-0.0210	-0.00081	0.00361	-0.00026
STORY1	28	WWIND	0.6877	0.0753	0.0133	-0.00084	0.00071	-0.00026
STORY1	29	WWIND	0.6744	0.0530	0.0193	-0.00015	0.00021	-0.00030
STORY1	30	WWIND	0.6668	0.0271	0.0133	0.00003	0.00019	-0.00026
STORY1	31	WWIND	0.6764	0.0017	0.0093	0.00011	0.00021	-0.00026
STORY1	32	WWIND	0.6897	-0.0075	0.0243	0.00097	0.00070	-0.00028
STORY1	33	WWIND	0.7216	-0.0308	0.0771	0.00084	0.00375	-0.00026
STORY1	34	WWIND	0.7470	-0.0436	-0.0697	0.00087	0.00391	-0.00026
STORY1	35	WWIND	0.7727	-0.0557	-0.0032	0.00115	0.00061	-0.00026
STORY1	36	WWIND	0.7987	-0.0672	0.0604	0.00099	0.00432	-0.00026
STORY1	37	WWIND	0.8250	-0.0779	-0.0558	0.00093	0.00441	-0.00026
STORY1	38	WWIND	0.8515	-0.0879	-0.0049	0.00085	0.00060	-0.00026
STORY1	39	WWIND	0.8784	-0.0972	0.0441	0.00101	0.00485	-0.00026
STORY1	40	WWIND	0.9055	-0.1058	-0.0395	0.00093	0.00494	-0.00026
STORY1	41	WWIND	0.9328	-0.1137	-0.0055	0.00061	0.00076	-0.00026
STORY1	42	WWIND	0.9604	-0.1208	0.0261	0.00097	0.00539	-0.00026
STORY1	43	WWIND	0.9880	-0.1271	-0.0210	0.00087	0.00546	-0.00026
STORY1	44	WWIND	1.0159	-0.1328	-0.0059	0.00031	0.00088	-0.00026
STORY1	45	WWIND	1.0439	-0.1376	0.0065	0.00087	0.00593	-0.00026
STORY1	46	WWIND	1.0720	-0.1418	-0.0008	0.00075	0.00595	-0.00026
STORY1	47	WWIND	1.1002	-0.1451	-0.0061	-0.00002	0.00095	-0.00026
STORY1	48	WWIND	1.1285	-0.1477	-0.0148	0.00070	0.00643	-0.00026
STORY1	49	WWIND	1.1569	-0.1496	0.0212	0.00057	0.00641	-0.00026
STORY1	50	WWIND	1.1853	-0.1507	-0.0058	-0.00038	0.00097	-0.00026
STORY1	51	WWIND	1.2137	-0.1510	-0.0375	0.00047	0.00691	-0.00026
STORY1	52	WWIND	1.2421	-0.1505	0.0452	0.00034	0.00684	-0.00026
STORY1	53	WWIND	1.2705	-0.1493	-0.0015	-0.00070	0.00086	-0.00026
STORY1	54	WWIND	1.2989	-0.1474	-0.0509	0.00029	0.00528	-0.00026
STORY1	55	WWIND	1.3271	-0.1446	0.0629	0.00009	0.00566	-0.00026
STORY1	56	WWIND	1.3553	-0.1411	0.0244	-0.00044	0.00062	-0.00026
STORY1	57	WWIND	1.3834	-0.1369	0.0117	-0.00009	0.00040	-0.00026
STORY1	58	WWIND	1.4114	-0.1319	0.0059	-0.00011	0.00037	-0.00026
STORY1	59	WWIND	1.4393	-0.1264	0.0010	-0.00010	0.00036	-0.00026
STORY1	60	WWIND	1.4668	-0.1195	-0.0023	-0.00009	0.00034	-0.00026
STORY1	61	WWIND	1.4934	-0.1100	-0.0009	0.00002	-0.00001	-0.00026

Appendix D.1 - ETABS Analysis Results

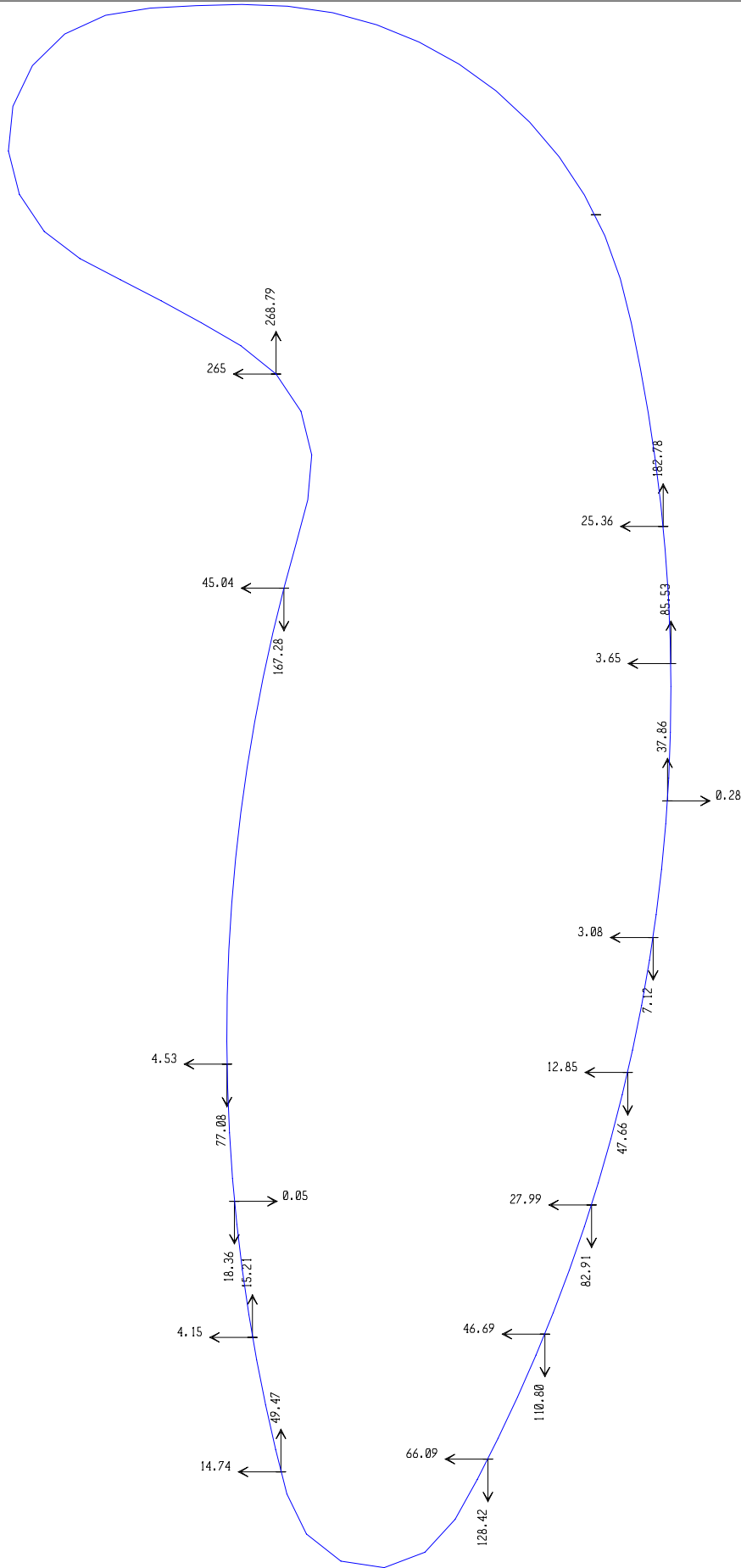
STORY1	62	WWIND	1.5188	-0.0972	-0.0012	0.00002	-0.00002	-0.00026
STORY1	63	WWIND	1.5425	-0.0816	-0.0036	-0.00015	0.00027	-0.00026
STORY1	64	WWIND	1.5702	-0.0591	-0.0017	-0.00010	0.00020	-0.00026
STORY1	65	WWIND	1.5833	-0.0424	0.0029	-0.00012	0.00022	-0.00026
STORY1	66	WWIND	1.5999	-0.0194	0.0094	-0.00011	0.00020	-0.00026
STORY1	67	WWIND	1.6137	0.0054	0.0178	-0.00008	0.00018	-0.00026
STORY1	68	WWIND	1.6244	0.0317	0.0272	-0.00006	0.00016	-0.00026
STORY1	69	WWIND	1.6318	0.0590	0.0376	-0.00002	0.00015	-0.00026
STORY1	70	WWIND	1.6359	0.0870	0.0484	0.00001	0.00015	-0.00026
STORY1	71	WWIND	1.6370	0.1154	0.0594	0.00002	0.00015	-0.00026
STORY1	72	WWIND	1.6363	0.1438	0.0704	0.00005	0.00015	-0.00026
STORY1	73	WWIND	1.6348	0.1722	0.0813	0.00003	0.00013	-0.00026
STORY1	74	WWIND	1.6303	0.2001	0.0852	-0.00001	0.00010	-0.00026
STORY1	75	WWIND	1.6187	0.2254	0.0958	0.00009	0.00022	-0.00026
STORY1	76	WWIND	1.5997	0.2456	0.1101	0.00015	0.00040	-0.00022
STORY1	77	WWIND	1.5738	0.2575	0.1219	0.00006	0.00045	-0.00026
STORY1	78	WWIND	1.5461	0.2603	0.1200	0.00006	0.00055	-0.00026
STORY1	79	WWIND	1.5191	0.2535	0.1011	0.00007	0.00054	-0.00026
STORY1	80	WWIND	1.4961	0.2381	0.0650	0.00034	0.00003	-0.00026
STORY1	81	WWIND	1.4872	0.2265	0.0511	0.00070	-0.00038	-0.00020
STORY1	82	WWIND	1.4661	0.1908	0.0594	0.00095	-0.00053	-0.00026
STORY1	83	WWIND	1.4531	0.1655	0.0746	0.00062	-0.00043	-0.00026
STORY1	84	WWIND	1.4395	0.1406	0.1275	-0.00076	-0.00068	-0.00026

ETABS v8.2.6 File: ETABS MODEL 2 (WITH RIGID DIAPHRAGM) Kip-in Units PAGE 2
November 7, 2003 18:11

AE 431W
3D ETABS Model

DISPLACEMENTS AT DIAPHRAGM CENTER OF MASS

STORY	DIAPHRAGM	LOAD	POINT	X	Y	UX	UY	RZ
STORY5	D1	WWIND	238	2322.834	-143.572	1.3870	0.0153	-0.00024
STORY4	D1	WWIND	239	2319.524	-143.617	1.3619	0.0162	-0.00024
STORY3	D1	WWIND	240	2320.417	-138.569	1.3248	0.0160	-0.00024
STORY2	D1	WWIND	241	2319.524	-143.617	1.2730	0.0159	-0.00025
STORY1	D1	WWIND	242	2317.821	-139.919	1.2058	0.0167	-0.00026



Appendix D.3 - ETABS Analysis Results

ETABS v8.2.6 File: ETABS MODEL 2 (WITH RIGID DIAPHRAGM AND RECENTERED LOAD) Kip-in Units PAGE 1
November 11, 2003 0:34

AE 431W
3D ETABS Model

P O I N T D I S P L A C E M E N T S

STORY	POINT	LOAD	UX	UY	UZ	RX	RY	RZ
STORY1	1	CENWIND	1.2178	0.0546	0.2228	-0.00044	0.00181	-0.00016
STORY1	2	CENWIND	1.2072	0.0414	0.0292	0.00090	0.00118	-0.00016
STORY1	3	CENWIND	1.1932	0.0321	-0.1470	-0.00065	0.00316	-0.00016
STORY1	4	CENWIND	1.1769	0.0280	-0.0750	-0.00040	-0.00061	-0.00016
STORY1	5	CENWIND	1.1601	0.0295	-0.0655	0.00016	-0.00007	-0.00016
STORY1	6	CENWIND	1.1436	0.0340	-0.0864	0.00027	0.00279	-0.00016
STORY1	7	CENWIND	1.1270	0.0385	-0.0096	-0.00053	0.00043	-0.00016
STORY1	8	CENWIND	1.1104	0.0426	0.0718	0.00024	0.00283	-0.00016
STORY1	9	CENWIND	1.0936	0.0462	0.0349	0.00030	0.00009	-0.00016
STORY1	10	CENWIND	1.0768	0.0495	0.0251	0.00004	0.00009	-0.00016
STORY1	11	CENWIND	1.0599	0.0523	0.0208	0.00004	0.00008	-0.00016
STORY1	12	CENWIND	1.0429	0.0546	0.0170	0.00004	0.00008	-0.00016
STORY1	13	CENWIND	1.0258	0.0566	0.0131	0.00004	0.00008	-0.00016
STORY1	14	CENWIND	1.0088	0.0580	0.0092	0.00004	0.00009	-0.00016
STORY1	15	CENWIND	0.9917	0.0591	0.0050	0.00003	0.00010	-0.00016
STORY1	16	CENWIND	0.9745	0.0597	-0.0006	0.00011	0.00026	-0.00016
STORY1	17	CENWIND	0.9574	0.0599	-0.0119	-0.00013	0.00409	-0.00016
STORY1	18	CENWIND	0.9402	0.0596	0.0065	-0.00021	0.00374	-0.00016
STORY1	19	CENWIND	0.9231	0.0589	0.0031	0.00000	0.00044	-0.00016
STORY1	20	CENWIND	0.9060	0.0577	0.0038	-0.00034	0.00501	-0.00016
STORY1	21	CENWIND	0.8889	0.0561	-0.0092	-0.00043	0.00499	-0.00016
STORY1	22	CENWIND	0.8719	0.0541	0.0032	-0.00025	0.00045	-0.00016
STORY1	23	CENWIND	0.8549	0.0516	0.0202	-0.00048	0.00471	-0.00016
STORY1	24	CENWIND	0.8380	0.0487	-0.0254	-0.00055	0.00466	-0.00016
STORY1	25	CENWIND	0.8212	0.0453	0.0022	-0.00048	0.00036	-0.00016
STORY1	26	CENWIND	0.8044	0.0416	0.0350	-0.00057	0.00438	-0.00016
STORY1	27	CENWIND	0.7878	0.0373	-0.0420	-0.00064	0.00385	-0.00016
STORY1	28	CENWIND	0.7728	0.0300	-0.0120	-0.00087	0.00055	-0.00016
STORY1	29	CENWIND	0.7637	0.0167	0.0014	-0.00009	-0.00003	-0.00016
STORY1	30	CENWIND	0.7602	0.0009	0.0101	0.00001	-0.00004	-0.00016
STORY1	31	CENWIND	0.7660	-0.0144	0.0191	0.00004	-0.00003	-0.00016
STORY1	32	CENWIND	0.7724	-0.0197	0.0368	0.00097	0.00057	-0.00016
STORY1	33	CENWIND	0.7933	-0.0340	0.0863	0.00090	0.00403	-0.00016
STORY1	34	CENWIND	0.8086	-0.0417	-0.0756	0.00095	0.00418	-0.00016
STORY1	35	CENWIND	0.8241	-0.0490	-0.0004	0.00107	0.00009	-0.00016
STORY1	36	CENWIND	0.8398	-0.0559	0.0675	0.00098	0.00443	-0.00016
STORY1	37	CENWIND	0.8556	-0.0624	-0.0613	0.00094	0.00454	-0.00016
STORY1	38	CENWIND	0.8717	-0.0685	-0.0029	0.00084	0.00018	-0.00016
STORY1	39	CENWIND	0.8879	-0.0741	0.0507	0.00094	0.00480	-0.00016
STORY1	40	CENWIND	0.9043	-0.0793	-0.0450	0.00087	0.00490	-0.00016
STORY1	41	CENWIND	0.9207	-0.0840	-0.0036	0.00062	0.00034	-0.00016
STORY1	42	CENWIND	0.9373	-0.0883	0.0330	0.00085	0.00517	-0.00016
STORY1	43	CENWIND	0.9541	-0.0921	-0.0271	0.00077	0.00524	-0.00016
STORY1	44	CENWIND	0.9709	-0.0955	-0.0039	0.00036	0.00046	-0.00016
STORY1	45	CENWIND	0.9878	-0.0985	0.0142	0.00072	0.00552	-0.00016
STORY1	46	CENWIND	1.0047	-0.1010	-0.0080	0.00062	0.00556	-0.00016
STORY1	47	CENWIND	1.0217	-0.1030	-0.0041	0.00007	0.00054	-0.00016
STORY1	48	CENWIND	1.0388	-0.1046	-0.0056	0.00055	0.00585	-0.00016
STORY1	49	CENWIND	1.0559	-0.1057	0.0123	0.00044	0.00584	-0.00016
STORY1	50	CENWIND	1.0731	-0.1063	-0.0038	-0.00024	0.00057	-0.00016
STORY1	51	CENWIND	1.0902	-0.1065	-0.0262	0.00034	0.00615	-0.00016
STORY1	52	CENWIND	1.1074	-0.1063	0.0339	0.00023	0.00610	-0.00016
STORY1	53	CENWIND	1.1245	-0.1055	-0.0001	-0.00051	0.00048	-0.00016
STORY1	54	CENWIND	1.1416	-0.1043	-0.0390	0.00020	0.00452	-0.00016
STORY1	55	CENWIND	1.1587	-0.1027	0.0509	0.00004	0.00488	-0.00016
STORY1	56	CENWIND	1.1757	-0.1006	0.0237	-0.00030	0.00028	-0.00016
STORY1	57	CENWIND	1.1926	-0.0980	0.0152	-0.00003	0.00008	-0.00016
STORY1	58	CENWIND	1.2095	-0.0950	0.0115	-0.00004	0.00007	-0.00016
STORY1	59	CENWIND	1.2263	-0.0917	0.0082	-0.00003	0.00007	-0.00016
STORY1	60	CENWIND	1.2429	-0.0875	0.0050	-0.00004	0.00006	-0.00016

Appendix D.3 - ETABS Analysis Results

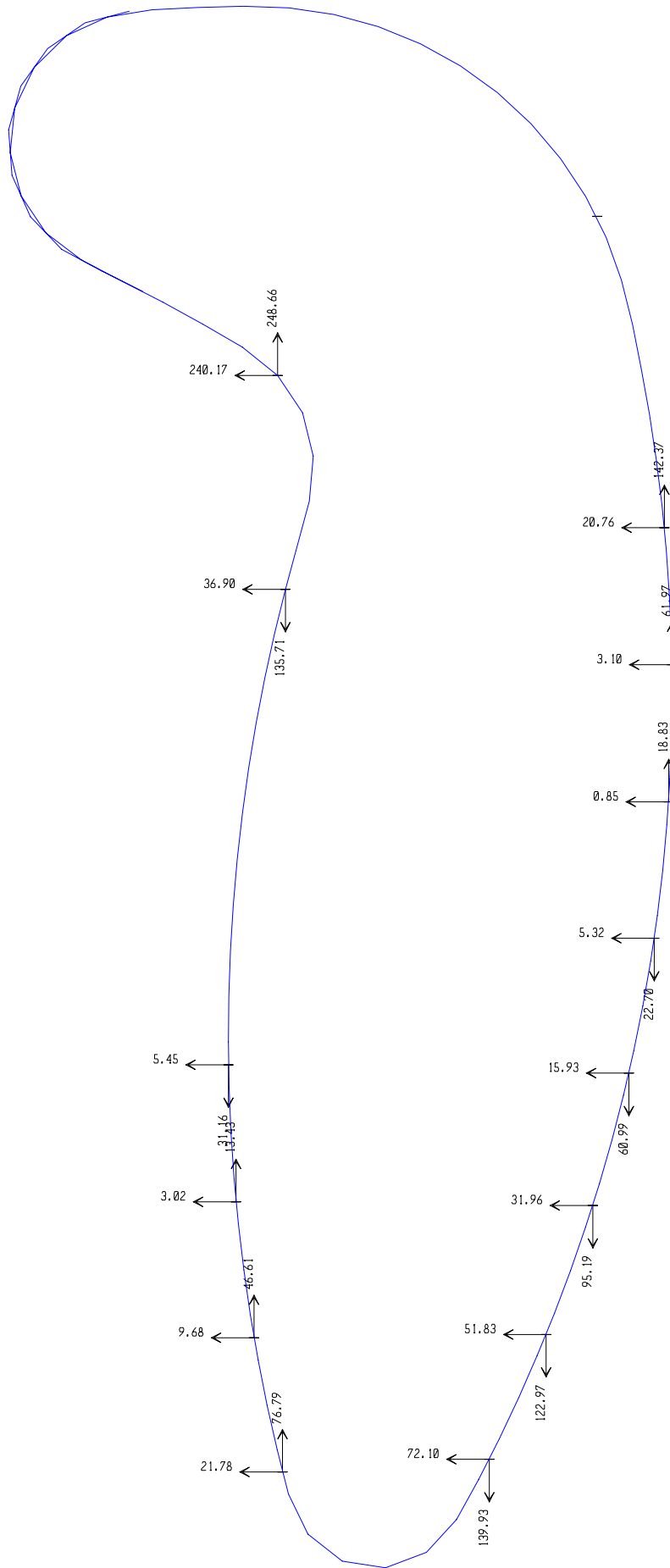
STORY1	61	CENWIND	1.2590	-0.0818	0.0016	-0.00010	0.00019	-0.00016
STORY1	62	CENWIND	1.2743	-0.0741	0.0006	-0.00010	0.00019	-0.00016
STORY1	63	CENWIND	1.2886	-0.0647	0.0020	-0.00002	0.00006	-0.00016
STORY1	64	CENWIND	1.3018	-0.0537	0.0029	-0.00002	0.00005	-0.00016
STORY1	65	CENWIND	1.3133	-0.0410	0.0043	-0.00002	0.00004	-0.00016
STORY1	66	CENWIND	1.3233	-0.0271	0.0059	-0.00001	0.00004	-0.00016
STORY1	67	CENWIND	1.3316	-0.0122	0.0079	-0.00001	0.00004	-0.00016
STORY1	68	CENWIND	1.3380	0.0037	0.0101	-0.00001	0.00003	-0.00016
STORY1	69	CENWIND	1.3425	0.0202	0.0125	0.00000	0.00003	-0.00016
STORY1	70	CENWIND	1.3450	0.0371	0.0150	0.00000	0.00003	-0.00016
STORY1	71	CENWIND	1.3456	0.0542	0.0176	0.00001	0.00003	-0.00016
STORY1	72	CENWIND	1.3452	0.0714	0.0202	0.00001	0.00003	-0.00016
STORY1	73	CENWIND	1.3443	0.0885	0.0226	0.00000	0.00003	-0.00016
STORY1	74	CENWIND	1.3416	0.1053	0.0236	-0.00001	0.00002	-0.00016
STORY1	75	CENWIND	1.3346	0.1206	0.0267	0.00000	0.00005	-0.00016
STORY1	76	CENWIND	1.3223	0.1329	0.0315	0.00002	0.00009	-0.00015
STORY1	77	CENWIND	1.3075	0.1400	0.0367	0.00000	0.00013	-0.00016
STORY1	78	CENWIND	1.2908	0.1416	0.0384	0.00000	0.00021	-0.00016
STORY1	79	CENWIND	1.2745	0.1375	0.0336	0.00001	0.00020	-0.00016
STORY1	80	CENWIND	1.2606	0.1282	0.0216	0.00017	-0.00010	-0.00016
STORY1	81	CENWIND	1.2528	0.1180	0.0244	0.00035	-0.00031	-0.00013
STORY1	82	CENWIND	1.2425	0.0997	0.0406	0.00043	-0.00036	-0.00016
STORY1	83	CENWIND	1.2347	0.0845	0.0612	0.00024	-0.00031	-0.00016
STORY1	84	CENWIND	1.2265	0.0694	0.1105	-0.00062	-0.00070	-0.00016
STORY1	255	CENWIND	1.0217	-0.0283	0.0000	0.00000	0.00000	-0.00016

ETABS v8.2.6 File: ETABS MODEL 2 (WITH RIGID DIAPHRAGM AND RECENTERED LOAD) Kip-in Units PAGE 2
November 11, 2003 0:34

AE 431W
3D ETABS Model

DISPLACEMENTS AT DIAPHRAGM CENTER OF MASS

STORY	DIAPHRAGM	LOAD	POINT	X	Y	UX	UY	RZ
STORY5	D1	CENWIND	261	2322.834	-143.572	1.1115	-0.0072	-0.00016
STORY4	D1	CENWIND	262	2319.524	-143.617	1.1064	-0.0066	-0.00016
STORY3	D1	CENWIND	263	2320.417	-138.569	1.1018	-0.0067	-0.00016
STORY2	D1	CENWIND	264	2319.524	-143.617	1.0964	-0.0065	-0.00016
STORY1	D1	CENWIND	265	2317.821	-139.919	1.0854	-0.0053	-0.00016



Appendix D.5 - ETABS Analysis Results

ETABS v8.2.6 File: ETABS MODEL 2 (WITH RIGID DIAPHRAGM AND RECENTERED LOAD 202) Kip-in Units PAGE 1
November 11, 2003 1:16

AE 431W
3D ETABS Model

P O I N T D I S P L A C E M E N T S

STORY	POINT	LOAD	UX	UY	UZ	RX	RY	RZ
STORY1	1	CENWIND	1.0409	-0.0009	0.1974	-0.00028	0.00153	-0.00006
STORY1	2	CENWIND	1.0366	-0.0063	0.0246	0.00083	0.00104	-0.00006
STORY1	3	CENWIND	1.0308	-0.0101	-0.1342	-0.00051	0.00273	-0.00006
STORY1	4	CENWIND	1.0242	-0.0117	-0.0667	-0.00038	-0.00058	-0.00006
STORY1	5	CENWIND	1.0173	-0.0111	-0.0553	0.00010	-0.00003	-0.00006
STORY1	6	CENWIND	1.0105	-0.0093	-0.0677	0.00029	0.00250	-0.00006
STORY1	7	CENWIND	1.0038	-0.0075	-0.0091	-0.00039	0.00037	-0.00006
STORY1	8	CENWIND	0.9970	-0.0058	0.0541	0.00027	0.00253	-0.00006
STORY1	9	CENWIND	0.9901	-0.0043	0.0261	0.00023	0.00009	-0.00006
STORY1	10	CENWIND	0.9832	-0.0030	0.0192	0.00003	0.00008	-0.00006
STORY1	11	CENWIND	0.9763	-0.0018	0.0165	0.00003	0.00007	-0.00006
STORY1	12	CENWIND	0.9694	-0.0009	0.0141	0.00003	0.00008	-0.00006
STORY1	13	CENWIND	0.9624	-0.0001	0.0117	0.00003	0.00008	-0.00006
STORY1	14	CENWIND	0.9554	0.0005	0.0092	0.00002	0.00008	-0.00006
STORY1	15	CENWIND	0.9484	0.0010	0.0067	0.00002	0.00009	-0.00006
STORY1	16	CENWIND	0.9414	0.0012	0.0039	0.00004	0.00024	-0.00006
STORY1	17	CENWIND	0.9344	0.0013	0.0007	0.00002	0.00402	-0.00006
STORY1	18	CENWIND	0.9274	0.0012	-0.0053	-0.00005	0.00366	-0.00006
STORY1	19	CENWIND	0.9204	0.0009	0.0038	-0.00017	0.00042	-0.00006
STORY1	20	CENWIND	0.9134	0.0004	0.0178	-0.00017	0.00508	-0.00006
STORY1	21	CENWIND	0.9064	-0.0003	-0.0232	-0.00026	0.00504	-0.00006
STORY1	22	CENWIND	0.8995	-0.0011	0.0032	-0.00043	0.00043	-0.00006
STORY1	23	CENWIND	0.8925	-0.0021	0.0344	-0.00033	0.00493	-0.00006
STORY1	24	CENWIND	0.8856	-0.0033	-0.0400	-0.00040	0.00486	-0.00006
STORY1	25	CENWIND	0.8787	-0.0047	0.0016	-0.00067	0.00033	-0.00006
STORY1	26	CENWIND	0.8719	-0.0062	0.0497	-0.00047	0.00476	-0.00006
STORY1	27	CENWIND	0.8651	-0.0079	-0.0584	-0.00050	0.00411	-0.00006
STORY1	28	CENWIND	0.8589	-0.0109	-0.0198	-0.00109	0.00067	-0.00006
STORY1	29	CENWIND	0.8560	-0.0167	-0.0032	-0.00011	-0.00004	-0.00006
STORY1	30	CENWIND	0.8538	-0.0228	0.0077	0.00001	-0.00006	-0.00006
STORY1	31	CENWIND	0.8562	-0.0291	0.0188	0.00005	-0.00005	-0.00006
STORY1	32	CENWIND	0.8548	-0.0271	0.0390	0.00107	0.00061	-0.00007
STORY1	33	CENWIND	0.8673	-0.0371	0.0943	0.00097	0.00437	-0.00006
STORY1	34	CENWIND	0.8736	-0.0403	-0.0827	0.00102	0.00454	-0.00006
STORY1	35	CENWIND	0.8799	-0.0432	-0.0004	0.00116	0.00008	-0.00006
STORY1	36	CENWIND	0.8863	-0.0461	0.0741	0.00097	0.00463	-0.00006
STORY1	37	CENWIND	0.8928	-0.0487	-0.0677	0.00093	0.00475	-0.00006
STORY1	38	CENWIND	0.8994	-0.0512	-0.0029	0.00092	0.00016	-0.00006
STORY1	39	CENWIND	0.9060	-0.0535	0.0569	0.00087	0.00485	-0.00006
STORY1	40	CENWIND	0.9127	-0.0556	-0.0510	0.00081	0.00496	-0.00006
STORY1	41	CENWIND	0.9194	-0.0575	-0.0035	0.00069	0.00031	-0.00006
STORY1	42	CENWIND	0.9262	-0.0593	0.0391	0.00075	0.00506	-0.00006
STORY1	43	CENWIND	0.9330	-0.0609	-0.0334	0.00067	0.00514	-0.00006
STORY1	44	CENWIND	0.9399	-0.0623	-0.0037	0.00044	0.00042	-0.00006
STORY1	45	CENWIND	0.9468	-0.0635	0.0210	0.00059	0.00525	-0.00006
STORY1	46	CENWIND	0.9538	-0.0645	-0.0151	0.00050	0.00529	-0.00006
STORY1	47	CENWIND	0.9607	-0.0653	-0.0038	0.00017	0.00049	-0.00006
STORY1	48	CENWIND	0.9677	-0.0659	0.0023	0.00041	0.00541	-0.00006
STORY1	49	CENWIND	0.9747	-0.0664	0.0038	0.00031	0.00542	-0.00006
STORY1	50	CENWIND	0.9817	-0.0667	-0.0035	-0.00012	0.00051	-0.00006
STORY1	51	CENWIND	0.9887	-0.0667	-0.0166	0.00021	0.00555	-0.00006
STORY1	52	CENWIND	0.9957	-0.0666	0.0234	0.00012	0.00551	-0.00006
STORY1	53	CENWIND	1.0027	-0.0663	-0.0006	-0.00038	0.00043	-0.00006
STORY1	54	CENWIND	1.0097	-0.0659	-0.0293	0.00010	0.00398	-0.00006
STORY1	55	CENWIND	1.0167	-0.0652	0.0393	-0.00003	0.00431	-0.00006
STORY1	56	CENWIND	1.0237	-0.0643	0.0183	-0.00024	0.00025	-0.00006
STORY1	57	CENWIND	1.0306	-0.0633	0.0117	-0.00002	0.00007	-0.00006
STORY1	58	CENWIND	1.0375	-0.0620	0.0088	-0.00003	0.00006	-0.00006
STORY1	59	CENWIND	1.0444	-0.0607	0.0062	-0.00003	0.00006	-0.00006

Appendix D.5 - ETABS Analysis Results

STORY1	60	CENWIND	1.0511	-0.0590	0.0038	-0.00003	0.00006	-0.00006
STORY1	61	CENWIND	1.0577	-0.0566	0.0012	-0.00008	0.00015	-0.00006
STORY1	62	CENWIND	1.0640	-0.0535	0.0005	-0.00008	0.00015	-0.00006
STORY1	63	CENWIND	1.0698	-0.0496	0.0016	-0.00002	0.00005	-0.00006
STORY1	64	CENWIND	1.0753	-0.0453	0.0025	-0.00002	0.00004	-0.00007
STORY1	65	CENWIND	1.0799	-0.0400	0.0037	-0.00001	0.00004	-0.00006
STORY1	66	CENWIND	1.0840	-0.0343	0.0051	-0.00001	0.00003	-0.00006
STORY1	67	CENWIND	1.0874	-0.0282	0.0069	-0.00001	0.00003	-0.00006
STORY1	68	CENWIND	1.0900	-0.0217	0.0088	0.00000	0.00003	-0.00006
STORY1	69	CENWIND	1.0919	-0.0149	0.0109	0.00000	0.00003	-0.00006
STORY1	70	CENWIND	1.0929	-0.0080	0.0131	0.00001	0.00003	-0.00006
STORY1	71	CENWIND	1.0931	-0.0010	0.0153	0.00001	0.00003	-0.00006
STORY1	72	CENWIND	1.0930	0.0060	0.0175	0.00001	0.00003	-0.00006
STORY1	73	CENWIND	1.0926	0.0130	0.0197	0.00001	0.00003	-0.00006
STORY1	74	CENWIND	1.0915	0.0199	0.0205	-0.00001	0.00002	-0.00006
STORY1	75	CENWIND	1.0886	0.0261	0.0232	0.00000	0.00004	-0.00006
STORY1	76	CENWIND	1.0834	0.0312	0.0274	0.00001	0.00008	-0.00006
STORY1	77	CENWIND	1.0775	0.0340	0.0319	0.00000	0.00011	-0.00006
STORY1	78	CENWIND	1.0707	0.0347	0.0335	0.00000	0.00018	-0.00006
STORY1	79	CENWIND	1.0641	0.0330	0.0293	0.00001	0.00018	-0.00006
STORY1	80	CENWIND	1.0584	0.0292	0.0188	0.00015	-0.00009	-0.00006
STORY1	81	CENWIND	1.0563	0.0265	0.0213	0.00031	-0.00027	-0.00004
STORY1	82	CENWIND	1.0510	0.0176	0.0357	0.00038	-0.00032	-0.00006
STORY1	83	CENWIND	1.0478	0.0113	0.0540	0.00021	-0.00028	-0.00006
STORY1	84	CENWIND	1.0444	0.0052	0.0976	-0.00055	-0.00063	-0.00006
STORY1	266	CENWIND	0.9358	-0.0348	0.0000	0.00000	0.00000	-0.00006

ETABS v8.2.6 File: ETABS MODEL 2 (WITH RIGID DIAPHRAGM AND RECENTERED LOAD 202) Kip-in Units PAGE 2
November 11, 2003 1:16

AE 431W
3D ETABS Model

DISPLACEMENTS AT DIAPHRAGM CENTER OF MASS

STORY	DIAPHRAGM	LOAD	POINT	X	Y	UX	UY	RZ
STORY5	D1	CENWIND	282	2322.834	-143.572	1.0085	-0.0269	-0.00007
STORY4	D1	CENWIND	283	2319.524	-143.617	1.0044	-0.0267	-0.00007
STORY3	D1	CENWIND	284	2320.417	-138.569	1.0005	-0.0266	-0.00007
STORY2	D1	CENWIND	285	2319.524	-143.617	0.9968	-0.0265	-0.00006
STORY1	D1	CENWIND	286	2317.821	-139.919	0.9868	-0.0254	-0.00006

Appendix D.6 - ETABS Analysis Results

ETABS v8.2.6 File: ETABS MODEL 2 (WITH RIGID DIAPHRAGM AND RECENTERED LOAD 221.2) Kip-in Units PAGE 1
November 11, 2003 1:32

AE 431W
3D ETABS Model

P O I N T D I S P L A C E M E N T S

STORY	POINT	LOAD	UX	UY	UZ	RX	RY	RZ
STORY1	1	CENWIND	0.9349	-0.0341	0.1822	-0.00018	0.00136	-0.00001
STORY1	2	CENWIND	0.9343	-0.0348	0.0218	0.00078	0.00095	-0.00001
STORY1	3	CENWIND	0.9336	-0.0353	-0.1266	-0.00043	0.00246	-0.00001
STORY1	4	CENWIND	0.9327	-0.0356	-0.0617	-0.00037	-0.00056	-0.00001
STORY1	5	CENWIND	0.9317	-0.0355	-0.0492	0.00007	0.00000	-0.00001
STORY1	6	CENWIND	0.9308	-0.0352	-0.0565	0.00031	0.00233	-0.00001
STORY1	7	CENWIND	0.9299	-0.0350	-0.0088	-0.00031	0.00033	-0.00001
STORY1	8	CENWIND	0.9290	-0.0348	0.0434	0.00029	0.00235	-0.00001
STORY1	9	CENWIND	0.9281	-0.0346	0.0209	0.00019	0.00010	-0.00001
STORY1	10	CENWIND	0.9272	-0.0344	0.0156	0.00002	0.00008	-0.00001
STORY1	11	CENWIND	0.9263	-0.0342	0.0139	0.00002	0.00007	-0.00001
STORY1	12	CENWIND	0.9253	-0.0341	0.0123	0.00002	0.00007	-0.00001
STORY1	13	CENWIND	0.9244	-0.0340	0.0108	0.00002	0.00007	-0.00001
STORY1	14	CENWIND	0.9235	-0.0339	0.0093	0.00002	0.00008	-0.00001
STORY1	15	CENWIND	0.9225	-0.0339	0.0077	0.00002	0.00009	-0.00001
STORY1	16	CENWIND	0.9216	-0.0338	0.0066	-0.00001	0.00023	-0.00001
STORY1	17	CENWIND	0.9207	-0.0338	0.0082	0.00010	0.00398	-0.00001
STORY1	18	CENWIND	0.9197	-0.0338	-0.0123	0.00005	0.00361	-0.00001
STORY1	19	CENWIND	0.9188	-0.0339	0.0042	-0.00027	0.00041	-0.00001
STORY1	20	CENWIND	0.9178	-0.0339	0.0262	-0.00007	0.00512	-0.00001
STORY1	21	CENWIND	0.9169	-0.0340	-0.0316	-0.00015	0.00506	-0.00001
STORY1	22	CENWIND	0.9160	-0.0341	0.0032	-0.00054	0.00042	-0.00001
STORY1	23	CENWIND	0.9150	-0.0343	0.0429	-0.00024	0.00506	-0.00001
STORY1	24	CENWIND	0.9141	-0.0344	-0.0488	-0.00031	0.00498	-0.00001
STORY1	25	CENWIND	0.9132	-0.0346	0.0012	-0.00078	0.00031	-0.00001
STORY1	26	CENWIND	0.9123	-0.0348	0.0584	-0.00041	0.00498	-0.00001
STORY1	27	CENWIND	0.9114	-0.0351	-0.0682	-0.00042	0.00427	-0.00001
STORY1	28	CENWIND	0.9106	-0.0355	-0.0245	-0.00122	0.00075	-0.00001
STORY1	29	CENWIND	0.9112	-0.0367	-0.0060	-0.00012	-0.00005	-0.00001
STORY1	30	CENWIND	0.9099	-0.0370	0.0063	0.00001	-0.00007	-0.00001
STORY1	31	CENWIND	0.9102	-0.0379	0.0186	0.00005	-0.00006	-0.00001
STORY1	32	CENWIND	0.9041	-0.0316	0.0404	0.00112	0.00064	-0.00001
STORY1	33	CENWIND	0.9117	-0.0390	0.0990	0.00101	0.00458	-0.00001
STORY1	34	CENWIND	0.9125	-0.0394	-0.0870	0.00107	0.00476	-0.00001
STORY1	35	CENWIND	0.9134	-0.0398	-0.0004	0.00122	0.00007	-0.00001
STORY1	36	CENWIND	0.9142	-0.0402	0.0781	0.00097	0.00475	-0.00001
STORY1	37	CENWIND	0.9151	-0.0405	-0.0714	0.00093	0.00488	-0.00001
STORY1	38	CENWIND	0.9160	-0.0408	-0.0029	0.00097	0.00015	-0.00001
STORY1	39	CENWIND	0.9169	-0.0412	0.0605	0.00084	0.00488	-0.00001
STORY1	40	CENWIND	0.9177	-0.0414	-0.0547	0.00078	0.00499	-0.00001
STORY1	41	CENWIND	0.9186	-0.0417	-0.0035	0.00074	0.00029	-0.00001
STORY1	42	CENWIND	0.9196	-0.0419	0.0428	0.00068	0.00500	-0.00001
STORY1	43	CENWIND	0.9205	-0.0421	-0.0372	0.00061	0.00508	-0.00001
STORY1	44	CENWIND	0.9214	-0.0423	-0.0036	0.00049	0.00040	-0.00001
STORY1	45	CENWIND	0.9223	-0.0425	0.0251	0.00051	0.00509	-0.00001
STORY1	46	CENWIND	0.9232	-0.0426	-0.0193	0.00042	0.00514	-0.00001
STORY1	47	CENWIND	0.9242	-0.0427	-0.0036	0.00022	0.00046	-0.00001
STORY1	48	CENWIND	0.9251	-0.0428	0.0071	0.00033	0.00515	-0.00001
STORY1	49	CENWIND	0.9260	-0.0429	-0.0012	0.00024	0.00517	-0.00001
STORY1	50	CENWIND	0.9270	-0.0429	-0.0034	-0.00005	0.00048	-0.00001
STORY1	51	CENWIND	0.9279	-0.0429	-0.0108	0.00014	0.00519	-0.00001
STORY1	52	CENWIND	0.9289	-0.0429	0.0172	0.00005	0.00516	-0.00001
STORY1	53	CENWIND	0.9298	-0.0429	-0.0009	-0.00030	0.00040	-0.00001
STORY1	54	CENWIND	0.9307	-0.0428	-0.0234	0.00005	0.00366	-0.00001
STORY1	55	CENWIND	0.9317	-0.0427	0.0323	-0.00008	0.00396	-0.00001
STORY1	56	CENWIND	0.9326	-0.0426	0.0151	-0.00020	0.00023	-0.00001
STORY1	57	CENWIND	0.9335	-0.0425	0.0097	-0.00002	0.00007	-0.00001
STORY1	58	CENWIND	0.9345	-0.0423	0.0073	-0.00003	0.00006	-0.00001
STORY1	59	CENWIND	0.9354	-0.0421	0.0051	-0.00002	0.00005	-0.00001

Appendix D.6 - ETABS Analysis Results

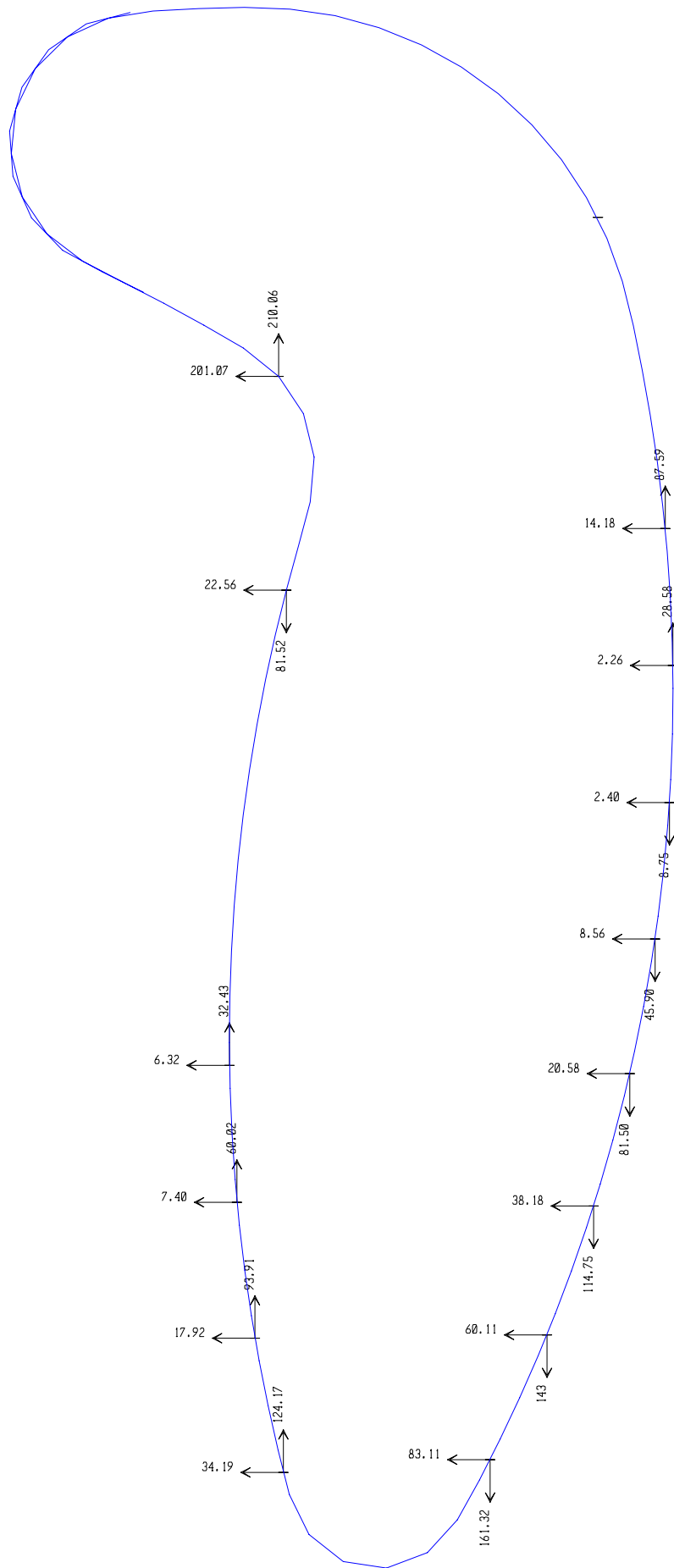
STORY1	60	CENWIND	0.9363	-0.0419	0.0031	-0.00003	0.00005	-0.00001
STORY1	61	CENWIND	0.9372	-0.0416	0.0010	-0.00006	0.00013	-0.00001
STORY1	62	CENWIND	0.9380	-0.0412	0.0004	-0.00006	0.00013	-0.00001
STORY1	63	CENWIND	0.9388	-0.0406	0.0015	-0.00001	0.00004	-0.00001
STORY1	64	CENWIND	0.9397	-0.0402	0.0023	-0.00001	0.00004	-0.00001
STORY1	65	CENWIND	0.9401	-0.0393	0.0034	-0.00001	0.00003	-0.00001
STORY1	66	CENWIND	0.9407	-0.0386	0.0047	-0.00001	0.00003	-0.00001
STORY1	67	CENWIND	0.9411	-0.0378	0.0063	0.00000	0.00003	-0.00001
STORY1	68	CENWIND	0.9415	-0.0369	0.0080	0.00000	0.00003	-0.00001
STORY1	69	CENWIND	0.9417	-0.0360	0.0100	0.00000	0.00003	-0.00001
STORY1	70	CENWIND	0.9419	-0.0351	0.0119	0.00001	0.00003	-0.00001
STORY1	71	CENWIND	0.9419	-0.0341	0.0139	0.00001	0.00003	-0.00001
STORY1	72	CENWIND	0.9419	-0.0332	0.0160	0.00001	0.00003	-0.00001
STORY1	73	CENWIND	0.9418	-0.0323	0.0179	0.00001	0.00002	-0.00001
STORY1	74	CENWIND	0.9417	-0.0313	0.0186	-0.00001	0.00002	-0.00001
STORY1	75	CENWIND	0.9413	-0.0305	0.0211	0.00001	0.00004	-0.00001
STORY1	76	CENWIND	0.9403	-0.0297	0.0249	0.00001	0.00007	0.00000
STORY1	77	CENWIND	0.9398	-0.0294	0.0291	0.00000	0.00010	-0.00001
STORY1	78	CENWIND	0.9389	-0.0293	0.0305	0.00000	0.00017	-0.00001
STORY1	79	CENWIND	0.9380	-0.0296	0.0267	0.00001	0.00016	-0.00001
STORY1	80	CENWIND	0.9372	-0.0301	0.0171	0.00014	-0.00008	-0.00001
STORY1	81	CENWIND	0.9387	-0.0283	0.0195	0.00029	-0.00025	0.00001
STORY1	82	CENWIND	0.9363	-0.0316	0.0328	0.00035	-0.00030	-0.00001
STORY1	83	CENWIND	0.9358	-0.0325	0.0496	0.00020	-0.00026	-0.00001
STORY1	84	CENWIND	0.9354	-0.0333	0.0899	-0.00050	-0.00058	-0.00001
STORY1	287	CENWIND	0.9188	-0.0386	0.0000	0.00000	0.00000	-0.00001

ETABS v8.2.6 File: ETABS MODEL 2 (WITH RIGID DIAPHRAGM AND RECENTERED LOAD 221.2) Kip-in Units PAGE 2
November 11, 2003 1:32

AE 431W
3D ETABS Model

DISPLACEMENTS AT DIAPHRAGM CENTER OF MASS

STORY	DIAPHRAGM	LOAD	POINT	X	Y	UX	UY	RZ
STORY5	D1	CENWIND	293	2322.834	-143.572	0.9469	-0.0388	-0.00001
STORY4	D1	CENWIND	294	2319.524	-143.617	0.9434	-0.0387	-0.00001
STORY3	D1	CENWIND	295	2320.417	-138.569	0.9398	-0.0386	-0.00001
STORY2	D1	CENWIND	296	2319.524	-143.617	0.9372	-0.0385	-0.00001
STORY1	D1	CENWIND	297	2317.821	-139.919	0.9277	-0.0374	-0.00001



Appendix E.1 - STAAD Analysis Results

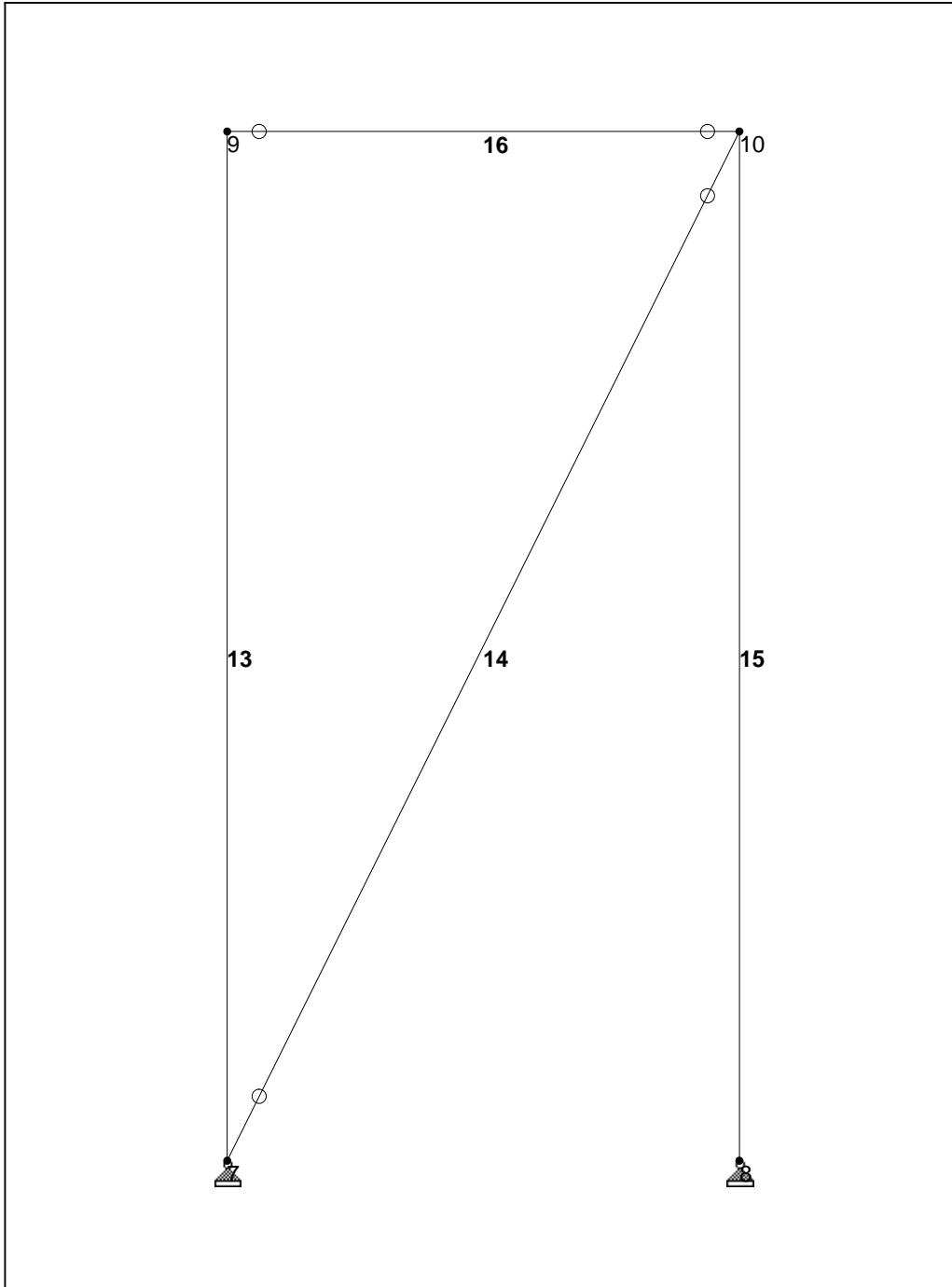


Software licensed to Authorizes User

Job No Technical Rep	Sheet No 1	Rev
Part	Ref	
By BJK	Date 09-Nov-03	Chd
Client	File BF1.std	Date/Time 11-Nov-2003 14:16

Job Title AE 431W

Client



Whole Structure

Appendix E.1 - STAAD Analysis Results



Software licensed to Authorizes User

Job No Technical Rep	Sheet No 2	Rev
Part		
Ref		
By BJK	Date 09-Nov-03	Chd
Client	File BF1.std	Date/Time 11-Nov-2003 14:16

Beam End Forces

Sign convention is as the action of the joint on the beam.

Beam	Node	L/C	Axial			Shear			Torsion	Bending	
			Fx (kip)	Fy (kip)	Fz (kip)	Mx (kip·ft)	My (kip·ft)	Mz (kip·ft)			
13	7	3:1.6 WIND	-0.000	0.000	0.000	0.000	0.000	0.000	0.000	-0.000	
	9	3:1.6 WIND	0.000	-0.000	0.000	0.000	0.000	0.000	0.000	-0.000	
14	7	3:1.6 WIND	-460.830	-0.000	0.000	0.000	0.000	0.000	0.000	0.000	
	10	3:1.6 WIND	460.830	0.000	0.000	0.000	0.000	0.000	0.000	0.000	
15	8	3:1.6 WIND	412.559	0.000	0.000	0.000	0.000	0.000	0.000	0.000	
	10	3:1.6 WIND	-412.559	-0.000	0.000	0.000	0.000	0.000	0.000	0.000	
16	9	3:1.6 WIND	205.328	-0.000	0.000	0.000	0.000	0.000	0.000	0.000	
	10	3:1.6 WIND	-205.328	0.000	0.000	0.000	0.000	0.000	0.000	0.000	

Appendix E.2 - STAAD Analysis Results

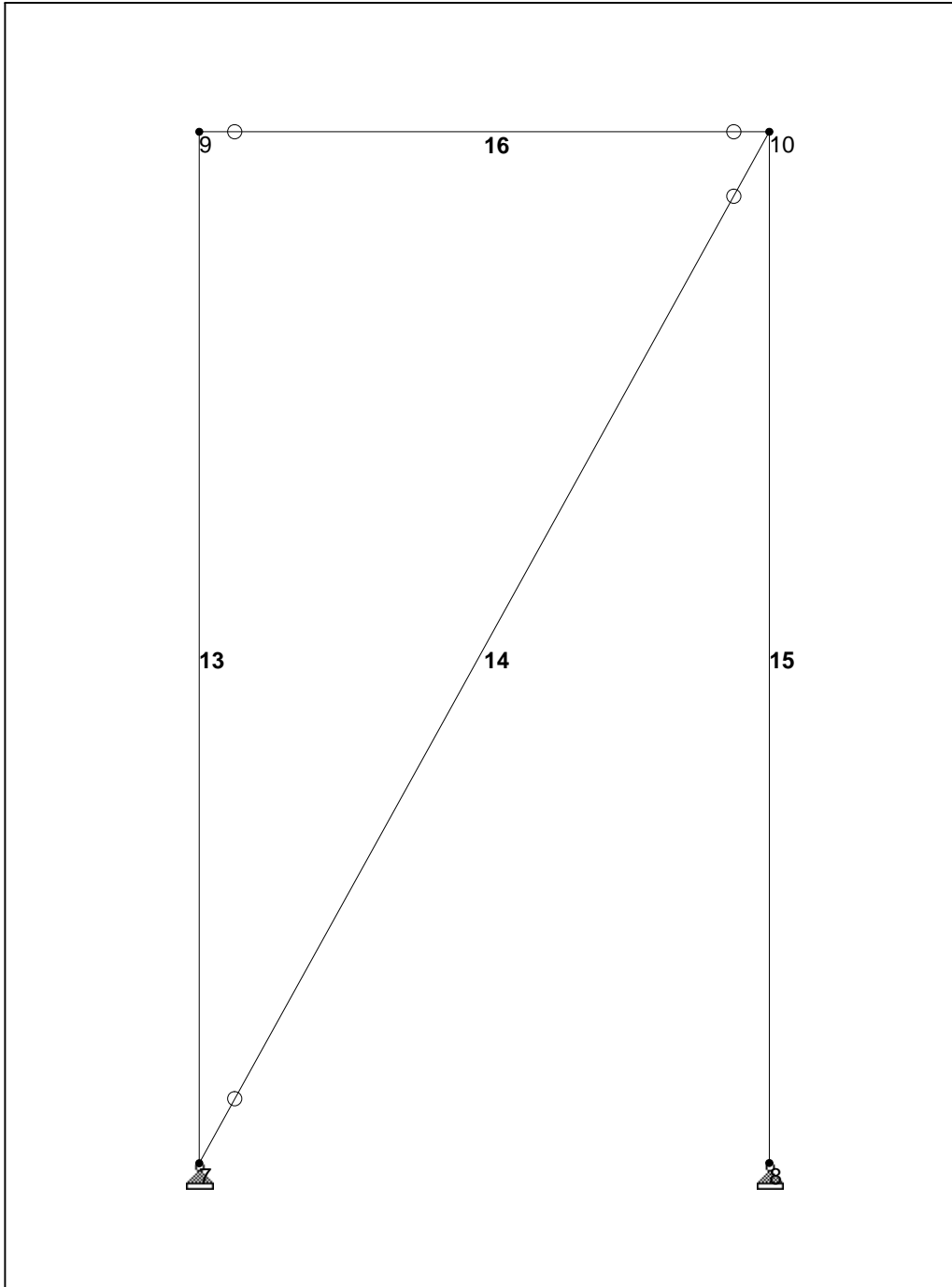


Software licensed to Authorizes User

Job No Technical Rep	Sheet No 1	Rev
Part	Ref	
By BJK	Date 09-Nov-03	Chd
Client	File BF4.std	Date/Time 11-Nov-2003 14:30

Job Title AE 431W

Client



Whole Structure

Appendix E.2 - STAAD Analysis Results

 Software licensed to Authorizes User	Job No	Sheet No	Rev
	Technical Rep	2	
Job Title AE 431W	Part		
	Ref		
	By BJB	Date 09-Nov-03	Chd
Client	File BF4.std	Date/Time 11-Nov-2003 14:30	

Beam End Forces

Sign convention is as the action of the joint on the beam.

Beam	Node	L/C	Axial	Shear		Torsion	Bending	
			Fx (kip)	Fy (kip)	Fz (kip)	Mx (kip·ft)	My (kip·ft)	Mz (kip·ft)
13	7	3:1.6 Wind	-0.000	0.000	0.000	0.000	0.000	-0.000
	9	3:1.6 Wind	0.000	-0.000	0.000	0.000	0.000	-0.000
14	7	3:1.6 Wind	-482.385	0.000	0.000	0.000	0.000	0.000
	10	3:1.6 Wind	482.385	-0.000	0.000	0.000	0.000	0.000
15	8	3:1.6 Wind	422.139	0.000	0.000	0.000	0.000	-0.000
	10	3:1.6 Wind	-422.139	-0.000	0.000	0.000	0.000	0.000
16	9	3:1.6 Wind	233.440	-0.000	0.000	0.000	0.000	0.000
	10	3:1.6 Wind	-233.440	0.000	0.000	0.000	0.000	0.000

Appendix F.1 - Diagrid Member Checking Spreadsheets

Member Properties - W14x82

ΦPn (tens.)	1080
ΦPn (comp.)	888
ΦMnx	6255
ΦMny	2016

Counts

CASE1	0
CASE2	6
CASE3	0
CASE4	46

Story	Beam	Load	Location in	Pu kip	Mux in-kip	Muy in-kip	Pu/ΦPn	H1-1a	H1-1b	Strength Utilization	Controlling Case
STORY5	B8	CASE1	0.0	0.00	129.90	0.00	0.000		X	0.021	CASE4
STORY5	B8	CASE1	21.6	0.00	74.30	0.00	0.000		X	0.012	
STORY5	B8	CASE1	43.2	0.00	18.69	0.00	0.000		X	0.003	
STORY5	B8	CASE1	64.8	0.00	-36.92	0.00	0.000		X	0.006	
STORY5	B8	CASE1	86.4	0.00	-92.53	0.00	0.000		X	0.015	
STORY5	B8	CASE1	108.0	0.00	-148.14	0.00	0.000		X	0.024	
STORY5	B8	CASE2	0.0	0.00	149.82	0.00	0.000		X	0.024	
STORY5	B8	CASE2	21.6	0.00	85.69	0.00	0.000		X	0.014	
STORY5	B8	CASE2	43.2	0.00	21.56	0.00	0.000		X	0.003	
STORY5	B8	CASE2	64.8	0.00	-42.58	0.00	0.000		X	0.007	
STORY5	B8	CASE2	86.4	0.00	-106.71	0.00	0.000		X	0.017	
STORY5	B8	CASE2	108.0	0.00	-170.84	0.00	0.000		X	0.027	
STORY5	B8	CASE3	0.0	0.00	131.71	0.00	0.000		X	0.021	
STORY5	B8	CASE3	21.6	0.00	75.33	0.00	0.000		X	0.012	
STORY5	B8	CASE3	43.2	0.00	18.94	0.00	0.000		X	0.003	
STORY5	B8	CASE3	64.8	0.00	-37.45	0.00	0.000		X	0.006	
STORY5	B8	CASE3	86.4	0.00	-93.83	0.00	0.000		X	0.015	
STORY5	B8	CASE3	108.0	0.00	-150.22	0.00	0.000		X	0.024	
STORY5	B8	CASE4	0.0	0.15	42.15	12.53	0.000		X	0.013	
STORY5	B8	CASE4	21.6	0.09	6.00	0.50	0.000		X	0.001	
STORY5	B8	CASE4	43.2	0.03	-30.15	-5.51	0.000		X	0.008	
STORY5	B8	CASE4	64.8	-0.03	-66.29	-5.51	0.000		X	0.013	
STORY5	B8	CASE4	86.4	-0.09	-102.44	0.50	0.000		X	0.017	
STORY5	B8	CASE4	108.0	-0.15	-138.59	12.53	0.000		X	0.028	
STORY3	B8	CASE1	0.0	0.00	243.58	0.00	0.000		X	0.039	CASE4
STORY3	B8	CASE1	21.6	0.00	140.65	0.00	0.000		X	0.022	
STORY3	B8	CASE1	43.2	0.00	37.72	0.00	0.000		X	0.006	
STORY3	B8	CASE1	64.8	0.00	-65.21	0.00	0.000		X	0.010	
STORY3	B8	CASE1	86.4	0.00	-168.14	0.00	0.000		X	0.027	
STORY3	B8	CASE1	108.0	0.00	-271.07	0.00	0.000		X	0.043	
STORY3	B8	CASE2	0.0	0.00	280.83	0.00	0.000		X	0.045	
STORY3	B8	CASE2	21.6	0.00	162.16	0.00	0.000		X	0.026	
STORY3	B8	CASE2	43.2	0.00	43.49	0.00	0.000		X	0.007	
STORY3	B8	CASE2	64.8	0.00	-75.19	0.00	0.000		X	0.012	
STORY3	B8	CASE2	86.4	0.00	-193.86	0.00	0.000		X	0.031	
STORY3	B8	CASE2	108.0	0.00	-312.53	0.00	0.000		X	0.050	
STORY3	B8	CASE3	0.0	0.00	247.17	0.00	0.000		X	0.040	
STORY3	B8	CASE3	21.6	0.00	142.72	0.00	0.000		X	0.023	
STORY3	B8	CASE3	43.2	0.00	38.27	0.00	0.000		X	0.006	
STORY3	B8	CASE3	64.8	0.00	-66.18	0.00	0.000		X	0.011	
STORY3	B8	CASE3	86.4	0.00	-170.63	0.00	0.000		X	0.027	
STORY3	B8	CASE3	108.0	0.00	-275.08	0.00	0.000		X	0.044	
STORY3	B8	CASE4	0.0	0.27	163.78	22.53	0.000		X	0.037	
STORY3	B8	CASE4	21.6	0.16	73.40	0.90	0.000		X	0.012	
STORY3	B8	CASE4	43.2	0.05	-16.99	-9.91	0.000		X	0.008	
STORY3	B8	CASE4	64.8	-0.05	-107.37	-9.91	0.000		X	0.022	
STORY3	B8	CASE4	86.4	-0.16	-197.75	0.90	0.000		X	0.032	
STORY3	B8	CASE4	108.0	-0.27	-288.14	22.53	0.000		X	0.057	
STORY1	B8	CASE1	0.0	0.00	586.75	0.00	0.000		X	0.094	CASE4
STORY1	B8	CASE1	21.6	0.00	303.16	0.00	0.000		X	0.048	
STORY1	B8	CASE1	43.2	0.00	19.56	0.00	0.000		X	0.003	
STORY1	B8	CASE1	64.8	0.00	-264.03	0.00	0.000		X	0.042	
STORY1	B8	CASE1	86.4	0.00	-547.63	0.00	0.000		X	0.088	
STORY1	B8	CASE1	108.0	0.00	-831.22	0.00	0.000		X	0.133	
STORY1	B8	CASE2	0.0	0.00	676.57	0.00	0.000		X	0.108	
STORY1	B8	CASE2	21.6	0.00	349.56	0.00	0.000		X	0.056	
STORY1	B8	CASE2	43.2	0.00	22.56	0.00	0.000		X	0.004	

Appendix F.2 - Diagrid Member Checking Spreadsheets

Member Properties - W12x87

ΦPn (tens.)	1152
ΦPn (comp.)	870
ΦMnx	5940
ΦMny	2718

Counts

CASE1	0
CASE2	24
CASE3	0
CASE4	64

Story	Beam	Load	Location in	Pu kip	Mux in-kip	Muy in-kip	Pu/ΦPn	H1-1a	H1-1b	Strength Utilization	Controlling Case
STORY5	D41	CASE1	0.0	-77.17	94.27	-0.01	0.089		X	0.060	CASE2
STORY5	D41	CASE1	84.9	-77.17	-8.20	-0.14	0.089		X	0.046	
STORY5	D41	CASE1	169.8	-77.17	-110.67	-0.26	0.089		X	0.063	
STORY5	D41	CASE2	0.0	-87.28	109.23	-0.02	0.100		X	0.069	
STORY5	D41	CASE2	84.9	-87.28	-9.45	-0.16	0.100		X	0.052	
STORY5	D41	CASE2	169.8	-87.28	-128.13	-0.30	0.100		X	0.072	
STORY5	D41	CASE3	0.0	-80.22	94.97	-0.01	0.092		X	0.062	
STORY5	D41	CASE3	84.9	-80.22	-8.32	-0.14	0.092		X	0.048	
STORY5	D41	CASE3	169.8	-80.22	-111.62	-0.26	0.092		X	0.065	
STORY5	D41	CASE4	0.0	-31.68	3.69	1.04	0.036		X	0.019	
STORY5	D41	CASE4	84.9	-31.68	-9.70	-0.02	0.036		X	0.020	
STORY5	D41	CASE4	169.8	-31.68	-23.09	-1.08	0.036		X	0.022	
STORY3	D41	CASE1	0.0	-119.35	67.30	0.91	0.137		X	0.080	CASE2
STORY3	D41	CASE1	84.9	-119.35	-5.95	0.26	0.137		X	0.070	
STORY3	D41	CASE1	169.8	-119.35	-79.20	-0.39	0.137		X	0.082	
STORY3	D41	CASE2	0.0	-138.23	77.40	1.05	0.159		X	0.093	
STORY3	D41	CASE2	84.9	-138.23	-6.86	0.30	0.159		X	0.081	
STORY3	D41	CASE2	169.8	-138.23	-91.12	-0.45	0.159		X	0.095	
STORY3	D41	CASE3	0.0	-122.54	67.82	0.92	0.141		X	0.082	
STORY3	D41	CASE3	84.9	-122.54	-6.04	0.26	0.141		X	0.072	
STORY3	D41	CASE3	169.8	-122.54	-79.90	-0.39	0.141		X	0.084	
STORY3	D41	CASE4	0.0	-115.01	-73.60	-27.71	0.132		X	0.089	
STORY3	D41	CASE4	84.9	-115.01	-23.11	-9.59	0.132		X	0.074	
STORY3	D41	CASE4	169.8	-115.01	27.38	8.53	0.132		X	0.074	
STORY5	D42	CASE1	0.0	57.72	-116.74	-0.33	0.050		X	0.045	CASE2
STORY5	D42	CASE1	84.9	57.72	3.66	0.12	0.050		X	0.026	
STORY5	D42	CASE1	169.8	57.72	124.06	0.58	0.050		X	0.046	
STORY5	D42	CASE2	0.0	68.28	-134.14	-0.38	0.059		X	0.052	
STORY5	D42	CASE2	84.9	68.28	4.22	0.14	0.059		X	0.030	
STORY5	D42	CASE2	169.8	68.28	142.58	0.66	0.059		X	0.054	
STORY5	D42	CASE3	0.0	56.55	-118.93	-0.33	0.049		X	0.045	
STORY5	D42	CASE3	84.9	56.55	3.71	0.13	0.049		X	0.025	
STORY5	D42	CASE3	169.8	56.55	126.35	0.58	0.049		X	0.046	
STORY5	D42	CASE4	0.0	11.42	-64.43	-1.98	0.010		X	0.017	
STORY5	D42	CASE4	84.9	11.42	-5.12	-0.17	0.010		X	0.006	
STORY5	D42	CASE4	169.8	11.42	54.20	1.63	0.010		X	0.015	
STORY3	D42	CASE1	0.0	25.18	-145.82	-1.09	0.022		X	0.036	CASE4
STORY3	D42	CASE1	84.9	25.18	-7.86	-0.24	0.022		X	0.012	
STORY3	D42	CASE1	169.8	25.18	130.11	0.61	0.022		X	0.033	
STORY3	D42	CASE2	0.0	28.40	-168.29	-1.25	0.025		X	0.041	
STORY3	D42	CASE2	84.9	28.40	-9.06	-0.27	0.025		X	0.014	
STORY3	D42	CASE2	169.8	28.40	150.18	0.71	0.025		X	0.038	
STORY3	D42	CASE3	0.0	24.08	-148.35	-1.10	0.021		X	0.036	
STORY3	D42	CASE3	84.9	24.08	-7.97	-0.24	0.021		X	0.012	
STORY3	D42	CASE3	169.8	24.08	132.40	0.62	0.021		X	0.033	
STORY3	D42	CASE4	0.0	-66.11	-152.49	25.49	0.076		X	0.073	
STORY3	D42	CASE4	84.9	-66.11	-23.72	8.90	0.076		X	0.045	
STORY3	D42	CASE4	169.8	-66.11	105.05	-7.68	0.076		X	0.059	
STORY5	D43	CASE1	0.0	-85.17	113.57	-0.28	0.098		X	0.068	CASE2
STORY5	D43	CASE1	84.9	-85.17	-6.47	-0.06	0.098		X	0.050	
STORY5	D43	CASE1	169.8	-85.17	-126.50	0.17	0.098		X	0.070	
STORY5	D43	CASE2	0.0	-96.50	131.48	-0.33	0.111		X	0.078	
STORY5	D43	CASE2	84.9	-96.50	-7.45	-0.07	0.111		X	0.057	
STORY5	D43	CASE2	169.8	-96.50	-146.39	0.19	0.111		X	0.080	
STORY5	D43	CASE3	0.0	-88.34	114.56	-0.29	0.102		X	0.070	
STORY5	D43	CASE3	84.9	-88.34	-6.56	-0.06	0.102		X	0.052	
STORY5	D43	CASE3	169.8	-88.34	-127.69	0.17	0.102		X	0.072	

Appendix F.3 - Diagrid Member Checking Spreadsheets

Member Properties - W14x53

ΦPn (tens.)	702
ΦPn (comp.)	526
ΦMnx	3920
ΦMny	990

Counts

CASE1	0
CASE2	13
CASE3	0
CASE4	29

Story	Beam	Load	Location in	Pu kip	Mux in-kip	Muy in-kip	Pu/ΦPn	H1-1a	H1-1b	Strength Utilization	Controlling Case
STORY5	B26	CASE1	0.0	0.00	-103.78	0.00	0.000		X	0.026	CASE4
STORY5	B26	CASE1	21.6	0.00	-65.35	0.00	0.000		X	0.017	
STORY5	B26	CASE1	43.2	0.00	-26.93	0.00	0.000		X	0.007	
STORY5	B26	CASE1	64.8	0.00	11.50	0.00	0.000		X	0.003	
STORY5	B26	CASE1	86.4	0.00	49.92	0.00	0.000		X	0.013	
STORY5	B26	CASE1	108.0	0.00	88.35	0.00	0.000		X	0.023	
STORY5	B26	CASE2	0.0	0.00	-119.69	0.00	0.000		X	0.031	
STORY5	B26	CASE2	21.6	0.00	-75.37	0.00	0.000		X	0.019	
STORY5	B26	CASE2	43.2	0.00	-31.04	0.00	0.000		X	0.008	
STORY5	B26	CASE2	64.8	0.00	13.29	0.00	0.000		X	0.003	
STORY5	B26	CASE2	86.4	0.00	57.61	0.00	0.000		X	0.015	
STORY5	B26	CASE2	108.0	0.00	101.94	0.00	0.000		X	0.026	
STORY5	B26	CASE3	0.0	0.00	-105.26	0.00	0.000		X	0.027	
STORY5	B26	CASE3	21.6	0.00	-66.30	0.00	0.000		X	0.017	
STORY5	B26	CASE3	43.2	0.00	-27.35	0.00	0.000		X	0.007	
STORY5	B26	CASE3	64.8	0.00	11.61	0.00	0.000		X	0.003	
STORY5	B26	CASE3	86.4	0.00	50.56	0.00	0.000		X	0.013	
STORY5	B26	CASE3	108.0	0.00	89.52	0.00	0.000		X	0.023	
STORY5	B26	CASE4	0.0	0.18	-73.89	-12.44	0.000		X	0.032	
STORY5	B26	CASE4	21.6	0.11	-46.08	-0.50	0.000		X	0.012	
STORY5	B26	CASE4	43.2	0.04	-18.27	5.47	0.000		X	0.010	
STORY5	B26	CASE4	64.8	-0.04	9.55	5.47	0.000		X	0.008	
STORY5	B26	CASE4	86.4	-0.11	37.36	-0.50	0.000		X	0.010	
STORY5	B26	CASE4	108.0	-0.18	65.17	-12.44	0.000		X	0.029	
STORY3	B26	CASE1	0.0	0.00	-162.75	0.00	0.000		X	0.042	
STORY3	B26	CASE1	21.6	0.00	-103.76	0.00	0.000		X	0.026	
STORY3	B26	CASE1	43.2	0.00	-44.76	0.00	0.000		X	0.011	
STORY3	B26	CASE1	64.8	0.00	14.23	0.00	0.000		X	0.004	
STORY3	B26	CASE1	86.4	0.00	73.23	0.00	0.000		X	0.019	
STORY3	B26	CASE1	108.0	0.00	132.22	0.00	0.000		X	0.034	
STORY3	B26	CASE2	0.0	0.00	-187.65	0.00	0.000		X	0.048	
STORY3	B26	CASE2	21.6	0.00	-119.63	0.00	0.000		X	0.031	
STORY3	B26	CASE2	43.2	0.00	-51.61	0.00	0.000		X	0.013	
STORY3	B26	CASE2	64.8	0.00	16.40	0.00	0.000		X	0.004	
STORY3	B26	CASE2	86.4	0.00	84.42	0.00	0.000		X	0.022	
STORY3	B26	CASE2	108.0	0.00	152.44	0.00	0.000		X	0.039	
STORY3	B26	CASE3	0.0	0.00	-165.18	0.00	0.000		X	0.042	
STORY3	B26	CASE3	21.6	0.00	-105.31	0.00	0.000		X	0.027	
STORY3	B26	CASE3	43.2	0.00	-45.43	0.00	0.000		X	0.012	
STORY3	B26	CASE3	64.8	0.00	14.45	0.00	0.000		X	0.004	
STORY3	B26	CASE3	86.4	0.00	74.33	0.00	0.000		X	0.019	
STORY3	B26	CASE3	108.0	0.00	134.20	0.00	0.000		X	0.034	
STORY3	B26	CASE4	0.0	0.32	-110.18	-22.36	0.000		X	0.051	
STORY3	B26	CASE4	21.6	0.19	-68.26	-0.89	0.000		X	0.018	
STORY3	B26	CASE4	43.2	0.06	-26.35	9.84	0.000		X	0.017	
STORY3	B26	CASE4	64.8	-0.06	15.58	9.84	0.000		X	0.014	
STORY3	B26	CASE4	86.4	-0.19	57.49	-0.89	0.000		X	0.016	
STORY3	B26	CASE4	108.0	-0.32	99.41	-22.36	0.001		X	0.048	
STORY1	B26	CASE1	0.0	0.00	-109.59	0.00	0.000		X	0.028	
STORY1	B26	CASE1	21.6	0.00	-96.02	0.00	0.000		X	0.024	
STORY1	B26	CASE1	43.2	0.00	-82.44	0.00	0.000		X	0.021	
STORY1	B26	CASE1	64.8	0.00	-68.86	0.00	0.000		X	0.018	
STORY1	B26	CASE1	86.4	0.00	-55.28	0.00	0.000		X	0.014	
STORY1	B26	CASE1	108.0	0.00	-41.71	0.00	0.000		X	0.011	
STORY1	B26	CASE2	0.0	0.00	-126.40	0.00	0.000		X	0.032	
STORY1	B26	CASE2	21.6	0.00	-110.73	0.00	0.000		X	0.028	
STORY1	B26	CASE2	43.2	0.00	-95.06	0.00	0.000		X	0.024	

Appendix F.4 - Diagrid Member Checking Spreadsheets

Member Properties - W12x50

ΦPn (tens.)	657
ΦPn (comp.)	360
ΦMnx	3236
ΦMny	959

Counts

CASE1	0
CASE2	14
CASE3	1
CASE4	57

Story	Beam	Load	Location in	Pu kip	Mux in-kip	Muy in-kip	Pu/ΦPn	H1-1a	H1-1b	Strength Utilization	Controlling Case	
STORY5	D77	CASE1	0.0	-50.50	58.18	0.33	0.140		X	0.088	CASE2	
STORY5	D77	CASE1	84.9	-50.50	-6.10	-0.35	0.140		X	0.072		
STORY5	D77	CASE1	169.8	-50.50	-70.38	-1.02	0.140		X	0.093		
STORY5	D77	CASE2	0.0	-56.53	67.63	0.37	0.157		X	0.100		
STORY5	D77	CASE2	84.9	-56.53	-7.03	-0.40	0.157		X	0.081		
STORY5	D77	CASE2	169.8	-56.53	-81.70	-1.18	0.157		X	0.105		
STORY5	D77	CASE3	0.0	-53.18	58.37	0.33	0.148		X	0.092		
STORY5	D77	CASE3	84.9	-53.18	-6.19	-0.35	0.148		X	0.076		
STORY5	D77	CASE3	169.8	-53.18	-70.76	-1.03	0.148		X	0.097		
STORY5	D77	CASE4	0.0	-38.84	41.91	0.27	0.108		X	0.067		
STORY5	D77	CASE4	84.9	-38.84	-3.84	-0.17	0.108		X	0.055		
STORY5	D77	CASE4	169.8	-38.84	-49.60	-0.61	0.108		X	0.070		
STORY3	D77	CASE1	0.0	-66.31	23.80	0.53	0.184		X	0.100		
STORY3	D77	CASE1	84.9	-66.31	-6.21	-0.17	0.184		X	0.094		
STORY3	D77	CASE1	169.8	-66.31	-36.22	-0.88	0.184		X	0.104		
STORY3	D77	CASE2	0.0	-77.08	27.23	0.61	0.214	X		0.222	CASE2	
STORY3	D77	CASE2	84.9	-77.08	-7.16	-0.20	0.214	X		0.216		
STORY3	D77	CASE2	169.8	-77.08	-41.56	-1.01	0.214	X		0.226		
STORY3	D77	CASE3	0.0	-68.73	23.66	0.54	0.191		X	0.103		
STORY3	D77	CASE3	84.9	-68.73	-6.31	-0.18	0.191		X	0.098		
STORY3	D77	CASE3	169.8	-68.73	-36.27	-0.89	0.191		X	0.108		
STORY3	D77	CASE4	0.0	-54.90	-4.93	-8.97	0.153		X	0.087		
STORY3	D77	CASE4	84.9	-54.90	-5.46	-3.67	0.153		X	0.082		
STORY3	D77	CASE4	169.8	-54.90	-6.00	1.63	0.153		X	0.080		
STORY5	D78	CASE1	0.0	30.98	-78.81	1.76	0.047		X	0.050		CASE4
STORY5	D78	CASE1	84.9	30.98	2.20	0.89	0.047		X	0.025		
STORY5	D78	CASE1	169.8	30.98	83.21	0.02	0.047		X	0.049		
STORY5	D78	CASE2	0.0	37.45	-90.37	2.03	0.057		X	0.059		
STORY5	D78	CASE2	84.9	37.45	2.54	1.03	0.057		X	0.030		
STORY5	D78	CASE2	169.8	37.45	95.44	0.02	0.057		X	0.058		
STORY5	D78	CASE3	0.0	29.44	-80.50	1.79	0.045		X	0.049		
STORY5	D78	CASE3	84.9	29.44	2.23	0.90	0.045		X	0.024		
STORY5	D78	CASE3	169.8	29.44	84.97	0.02	0.045		X	0.049		
STORY5	D78	CASE4	0.0	20.03	-58.35	0.79	0.030		X	0.034		
STORY5	D78	CASE4	84.9	20.03	1.00	0.45	0.030		X	0.016		
STORY5	D78	CASE4	169.8	20.03	60.34	0.11	0.030		X	0.034		
STORY3	D78	CASE1	0.0	-20.34	-82.61	0.83	0.057		X	0.055	CASE4	
STORY3	D78	CASE1	84.9	-20.34	-2.42	0.53	0.057		X	0.030		
STORY3	D78	CASE1	169.8	-20.34	77.77	0.23	0.057		X	0.053		
STORY3	D78	CASE2	0.0	-24.08	-95.43	0.95	0.067		X	0.064		
STORY3	D78	CASE2	84.9	-24.08	-2.79	0.61	0.067		X	0.035		
STORY3	D78	CASE2	169.8	-24.08	89.85	0.27	0.067		X	0.061		
STORY3	D78	CASE3	0.0	-22.11	-84.24	0.84	0.061		X	0.058		
STORY3	D78	CASE3	84.9	-22.11	-2.46	0.54	0.061		X	0.032		
STORY3	D78	CASE3	169.8	-22.11	79.33	0.24	0.061		X	0.055		
STORY3	D78	CASE4	0.0	-25.58	-60.91	18.72	0.071		X	0.074		
STORY3	D78	CASE4	84.9	-25.58	-5.53	6.08	0.071		X	0.044		
STORY3	D78	CASE4	169.8	-25.58	49.86	-6.55	0.071		X	0.058		
STORY5	D79	CASE1	0.0	-63.84	73.44	2.16	0.177		X	0.114		CASE2
STORY5	D79	CASE1	84.9	-63.84	-5.48	-2.93	0.177		X	0.093		
STORY5	D79	CASE1	169.8	-63.84	-84.39	-8.03	0.177		X	0.123		
STORY5	D79	CASE2	0.0	-71.90	85.20	2.49	0.200		X	0.129		
STORY5	D79	CASE2	84.9	-71.90	-6.31	-3.39	0.200		X	0.105		
STORY5	D79	CASE2	169.8	-71.90	-97.83	-9.26	0.200		X	0.140		
STORY5	D79	CASE3	0.0	-66.73	73.88	2.20	0.185		X	0.118		
STORY5	D79	CASE3	84.9	-66.73	-5.57	-2.98	0.185		X	0.098		
STORY5	D79	CASE3	169.8	-66.73	-85.03	-8.16	0.185		X	0.127		